NOTICE

The quality of this microform is heavily dependent upon the quality of the original thesis submitted for microfilming. Every effort has been made to ensure the highest quality of reproduction possible.

If pages are missing, contact the university which granted the degree.

Some pages may have indistinct print especially if the original pages were typed with a poor typewriter ribbon or if the university sent us an inferior photocopy.

Reproduction in full or in part of this microform is governed by the Canadian Copyright Act, R.S.C. 1970, c. C-30, and subsequent amendments.

AVIS

La qualité de cette microforme dépend grandement de la qualité de la thèse soumise au microfilmage. Nous avons tout fait pour assurer une qualité supérieure de reproduction.

S'il manque des pages, veuillez communiquer avec l'université qui a conféré le grade.

La qualité d'impression de certaines pages peut laisser à désirer, surtout si les pages originales ont été dactylographiées à l'aide d'un ruban usé ou si l'université nous a fait parvenir une photocopie de qualité inférieure.

La reproduction, même partielle, de cette microforme est soumise à la Loi canadienne sur le droit d'auteur, SRC 1970, c. C-30, et ses amendements subséquents.

Feature Extraction and Reconstruction of Two Dimensional Patterns using Autoregressive Moving Average Models and Fourier Descriptors

Siu Yun Leung

A Thesis
in
The Department
of
Mathematics and Statistics

Presented in Partial Fulfillment of the Requirements for
the Degree of Master of Science at
Concordia University
Montréal, Québec, Canada

September 1989

ISBN 0-315-51309-8

Abstract

Feature Extraction and Reconstruction
of Two Dimensional Patterns using
Autoregressive Moving Average Models and Fourier Descriptors

Siu Yun Leung

The analysis of closed boundaries of arbitrary shapes on a plane is discussed. Specifically, the problems of representation and reconstruction are considered. In the first part, circular autoregressive moving average model is suggested for the representation of the sequence of numbers derived from the closed boundary. The stochastic model is invariant to transformations such as scaling, translations, and shifts of the starting point. A method for estimating the parameters of the model is given and a decision rule for choosing the appropriate order is also included. In the second part, modifications and improvements of Fourier descriptors, which are defined by Zahn and Roskies are proposed. The amplitudes of the Fourier descriptors are shown to be invariant under rotations, translations, scaling, mirror reflections and shifts of the starting point. For both parts, reconstruction of curves are discussed and the results of simulation is also presented.

To my family and

the memory of my uncle Chi Hung Leung

Acknowledgements

I would like to take this chance to express my appreciation to my advisor Professor A. Krzyzak for his support, encouragement and advice in the preparation and composition of this thesis and permitting me to use his Personal Computer for the preparation of this final copy of my thesis by using the LaTeX package. Professor A. Krzyzak has taught me much, not only about computer science, mathematics, statistics and analysis, but also the rewards in research and the pursuit of knowledge. I feel forunate to have had Professor A. Krzyzak as my thesis advisor. I am very grateful to Professor C.Y. Suen for very useful and helpful discussions.

I am also grateful for the financial assistant provided by Professor A. Krzyzak, Professor C.Y. Suen and the Department of Mathematics and Statistics.

Finally, many thanks to the families of J.K. Chai, S.L. Cheung, Y.H. Lee and Y.K. Lee. Special thanks to Professor B.C. Desai, A. Fung, Y.T. Lee, N. Su, L. Tom and W. Wong.

This work has been supported in part by grants from the Natural Sciences and Engineering Research Council of Canada and the Department of Education of Québec.

Contents

List of Figures

List of Tables

Chapter 1

Introduction and Summary

In many applications of pattern recognition and digital image analysis, the shape of a simple connected object is represented by its contour. Different approaches have been proposed for two dimensional contour analysis, they include statistical approaches [9], [29], Fourier descriptors approaches [8], [18], [24], [25], [26], [27], [37], [45] and syntactic approaches [14], for a complete review refer to Mantas [30]. This thesis contains two parts. In the first part, the statistical approach is discussed. The given contour is approximated by a series of straight line segments and the coordinates on the contour are used for the representation. One of the characteristic of the data is its circularity. The observations are represented by an appropriate stochastic model belonging to the family of circular autoregressive moving average models. Every model is characterized by a set of unknown parameters and independent noise sequence. The parameters of the model corresponding to a given boundary are invariant to transformations of the boundary such as translations and shifts of the starting point. By suitable assumptions about the noise, expressions are obtained for the maximum likelihood estimates of the parameters of the model for the given boundary, see Chapter 3. In actual applications, the least squares estimates are used. The estimates are invariant to the transformations of the boundaries. An algorithm is presented to generate a closed boundary from the stored estimates of the parameters of the model. The main aim of the approach developed here is to demonstrate that stochastic models can be useful in representation a class of closed boundaries. Kashyap and Chellappa [21] used circular autoregressive models (CAR) to represent closed contours. By using Akaike Infor-

mation Criterion (AIC), we found that, in practice, the boundary sequences would be represented by the circular autoregressive moving average model (CARMA). That motivated us to consider CARMA models of general order for contour coding and reconstruction. CAR models of [21] are special cases of our model. In Chapter 4, we show that parameters of the models are invariant to translations, scaling and shifts of the starting point which are multiple of L/N, where L is the perimeter of the contour and N is the number of observations obtained from the boundary.

In the second part, the Fourier series approach for contour coding is discussed. Fourier descriptors are distinguished by their invariance to affine shape transformations such as scaling, rotations, translations, mirror reflections and shifts of the starting point. In the literature, the popularity of Granlund descriptors [18] far exceeds that of the Zahn and Roskies descriptors [45]. The reason is the discontinuity of the polygonal signature resulting from Zahn and Roskies method (ZR) which causes the Fourier coefficients to decrease slowly. The major drawbacks of Fourier descriptors lie in their insensitivity to spurs on the boundary (for instance, it is difficult to distinguish O from Q by using Fourier descriptors alone). On the other hand, this property may be useful in filtering out noise on the boundary. In order to improve the rate of decline of Fourier coefficients, we smooth the polygonal boundary and derive new SZR and LSZR type descriptors [24], [26]. ZR descriptors of Zahn and Roskies [45] are derived from an angular bend function signature of a contour. The signature for the polygonal contours has jump discontinuities corresponding to the vertices of the polygon but is simpler than the signature for ZR descriptors which is linearized so that $\phi^*(2\pi) = \phi^*(0) = 0$ but still has jump discontinuities corresponding to the vertices, where ϕ^* is the linearized step signature. It is well known that the partial Fourier series derived from the discontinuous function does not converge uniformly due to Gibb's phenomenon at the jump points, therefore signature with a controlled degree of smoothing is introduced. The smoothed signature, $\tilde{\phi}$, for SZR descriptors is obtained by smoothing the step polygonal signature resulting in absence of jump discontinuities at the vertices but we still have $\tilde{\phi}(2\pi) \neq \tilde{\phi}(0)$. The linearized, smoothed signature, $\tilde{\phi}^*$, for LSZR descriptors is obtained by linearizing the SZR signature so

that $\tilde{\phi}^*(2\pi) = \varphi^*(0)$, and in effect $\tilde{\phi}^*$ is continuous everywhere. As a result, the LSZR descriptors are the best among four different kinds of descriptors, see Chapter 6. These conclusions are not surprising. The negative effect of discontinuities in polygonal signatures is removed from LSZR signature and resulting descriptors. In particular the Gibb's phenomenon does not occur in $\tilde{\phi}^*$, since it is continuous everywhere and the corresponding Fourier series converges to $\tilde{\phi}^*$ uniformly. The invariance of amplitudes of all kinds of descriptors to translations, scaling and shifts of the starting point are shown in Chapter 5.

Two kinds of shape descriptors considered in this thesis based on stochastic models and Fourier coefficients share invariance properties. The choice of descriptors should be based on particular application. If considered contours contain substantial amount of noise stochastic approach is recommanded. On the other hand, Fourier descriptors are recommended in case of smooth shapes with slowly varying boundaries. The shape descriptors studied in this thesis will be applied in the future to classification of two dimensional objects.

Chapter 2

Stochastic Approach

In this chapter, statistical approach for time series modeling of closed contours is presented. We only consider discrete systems, that is the observations are available at discrete, equispaced instants of time. The time series is denoted by $z_1, \ldots, z_N$, where N is the total number of observations and z_i is the value of the observation at time i.

2.1 Representation of Closed Boundaries

The given closed boundary is represented by a finite sequence of real numbers, the time series. It is assumed that the boundary has no crossovers and is approximated by a polygon of N sides. The integer N is large enough to obtain the desired accuracy of the approximation. Among many methods to obtain the time series from the boundary, we will consider the one described below.

Consider a Cartesian coordinate system such that the centroid of the object is at the origin as shown in Figure 2.1. Let the perimeter of the polygon be L and let us take N equispaced points on the boundary with coordinates $(x_i, y_i), i = 1, \ldots, N$, and the distance (L/N) between any two consecutive points. The resulting time series is $\{(x_i, y_i), i = 1, \ldots, N\}$.

Another possible representation for closed smooth boundaries is the tangent angle versus arc length [24], [25], [26], [45], which will be disscussed in Chapter 5.

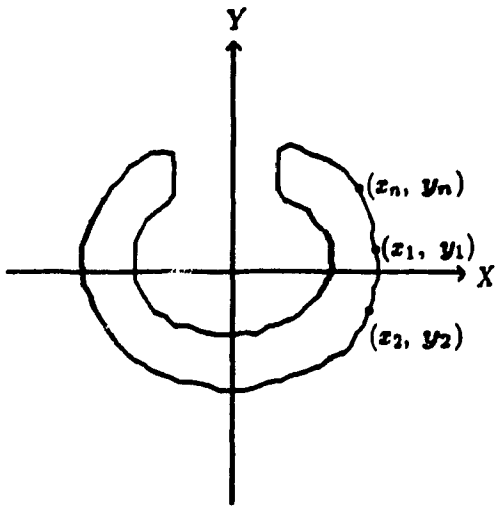

Figure 2.1: Two Dimensional Representation.

2.2 Mathematical Modeling of Boundaries

In the following section, we will define a number of quantities essential for our stochastic model.

2.2.1 Stochastic Process

A statistical phenomenon that evolves in time according to probabilistic laws is called a stochastic process. A special class of stochastic processes useful for describing time series is stationary process, that is the process which remains in equilibrium about a constant mean level.

Stationary Process

The stationary process is assumed to be in a specific form of statistical equilibrium, and in particular, to vary about a fixed mean. A stochastic process is said to be *strictly stationary* if its properties are unaffected by the change of time origin or more precisely

Definition 2.1 *The process $\{W_t\}$ is said to be strictly stationary if, for any admissible $t_1, \ldots, t_n$ and k, the joint probability distribution of $W_{t_1}, \ldots, W_{t_n}$ is identical with the joint probability distribution of $W_{t_1+k}, \ldots, W_{t_n+k}$.*

Strict stationarity is, however, a severe restriction, we therefore introduce the notion of 'stationarity up to order 2', which is a weaker condition but nevertheless describes roughly the same type of physical behaviour. This leads to the following definition

Definition 2.2 *The process $\{W_t\}$ is said to be stationary up to order 2 if for any admissible $t_1, \ldots, t_n$ and any k, all the joint moments up to order 2 of $\{W_{t_1}, \ldots, W_{t_n}\}$ exist and equal the corresponding joint moments up to order 2 of $\{W_{t_1+k}, \ldots, W_{t_n+k}\}$.*

Since multivariate Normal distribution is fully characterized by its first and second order moments, thus, an assumption of Normality plus second order stationarity, is sufficient for strictly stationarity.

Mean, Variance and Autocovariance

When $n = 1$, the strict stationarity assumption implies that the probability distribution of W_t is the same for all t so that the stochastic process has a constant mean, μ, and variance, σ_W^2.

The mean defines the level about which the process fluctuates and the variance measures its spread about this level. The strict stationarity assumption also implies that the joint probability distribution of W_t and W_{t+k} is the same for all times $t, t+k$ for any constant k.

Definition 2.3 *The autocovariance at lag k is defined by*

$$\gamma_k = E[(W_t - \mu)(W_{t+k} - \mu)].$$

Stationarity implies that γ_k is independent of t but not of k and it measures the covariance between W_t and W_{t+k}.

Definition 2.4 *The autocorrelation at lag k is defined by*

$$\rho_k = \frac{\gamma_k}{\gamma_0}.$$

Autocovariance Generating Function

The definitions of backward and forward shift operators are given below

Definition 2.5 *The backward shift operator is defined by*

$$B^j W_t = W_{t-j} \quad \text{for all integers } j.$$

Definition 2.6 *The forward shift operator is defined by*

$$F^j W_t = W_{t+j} \quad \text{for all integers } j.$$

Definition 2.7 *The autocovariance generating function is defined by*

$$\gamma(B) = \sum_{k=-\infty}^{\infty} \gamma_k B^k$$

where γ_k, the autocovariance of lag k, is the coefficient of both B^j and $B^{-j} = F^j$.

For a given linear process

$$W_t = \sum_{j=0}^{\infty} \psi_j Z_{t-j}$$

where Z_t's are uncorrelated random variables with $E[Z_t] = 0$, $var[Z_t] = \sigma_Z^2$ and ψ_j's are constants with $\psi_0 = 1$, the autocovariance at lag k of the process is

$$\begin{aligned} \gamma_k &= E[W_t W_{t+k}] \\ &= E[\sum_{j=0}^{\infty} \sum_{h=0}^{\infty} \psi_j \psi_h Z_{t-j} Z_{t+k-h}] \\ &= \sigma_Z^2 \sum_{j=0}^{\infty} \psi_j \psi_{j+k}. \end{aligned}$$

Substituting this result into the autocovariance generating function, we have

$$\begin{aligned} \gamma(B) &= \sigma_Z^2 \sum_{k=-\infty}^{\infty} \sum_{j=0}^{\infty} \psi_j \psi_{j+k} B^k \\ &= \sigma_Z^2 \sum_{j=0}^{\infty} \sum_{k=-j}^{\infty} \psi_j \psi_{j+k} B^k \end{aligned}$$

because $\psi_h = 0$ for $h < 0$. Writing $j + k = h$, so that $k = h - j$,

$$\begin{aligned} \gamma(B) &= \sigma_Z^2 \sum_{j=0}^{\infty} \sum_{h=0}^{\infty} \psi_j \psi_h B^{h-j} \\ &= \sigma_Z^2 \sum_{h=0}^{\infty} \psi_h B^h \sum_{j=0}^{\infty} \psi_j B^{-j}, \end{aligned}$$

$$\gamma(B) = \sigma_Z^2 \psi(B)\psi(B^{-1}) = \sigma_Z^2 \psi(B)\psi(F) \tag{2.1}$$

where

$$\psi(B) = \sum_{h=0}^{\infty} \psi_h B^h.$$

This shows that the generating function can be expressed as a function of forward and backward shift operators.

Linear Models for Time Series

There are several types of stochastic processes which are useful in setting up a model for time series such as autoregressive process, moving average process and autoregressive moving average process. The definitions are given below

Definition 2.8 *The process $\{Z_t\}, t = 0, \pm 1, \pm 2, \ldots$ is called a purely random process if it consists of a sequence of uncorrelated random variables, i.e., if for all $s \neq t$, $cov[Z_s, Z_t] = 0$.*

Definition 2.9 *$\{W_t\}$ is an autoregressive process of order p (denoted by AR(p)) if it satisfies*

$$W_t - \phi_1 W_{t-1} - \cdots - \phi_p W_{t-p} = Z_t$$

where $\phi_1, \ldots, \phi_p$ are constants and $\{Z_t\}$ is a purely random process.

The equation can be written concisely in the form

$$\phi(B) W_t = Z_t$$

where

$$\phi(B) = 1 - \phi_1 B - \cdots - \phi_p B^p$$

and the process is stationary if zeroes of the characteristic equation $\phi(B) = 0$ lie outside the unit circle.

Definition 2.10 *$\{W_t\}$ is a moving average process of order q (denoted by MA(q)) if it satisfies*

$$W_t = Z_t - \theta_1 Z_{t-1} - \cdots - \theta_q Z_{t-q}$$

where $\theta_1, \ldots, \theta_q$ are constants and $\{Z_t\}$ is a purely random process.

The equation can be written in the form

$$W_t = \theta(B)Z_t$$

where

$$\theta(B) = 1 - \theta_1 B - \cdots - \theta_q B^q$$

and the process is invertible if zeroes of the characteristic equation $\theta(F) = 0$ lie outside the unit circle. It is natural to combine the autoregressive and moving average models to construct a more general model which is known as autoregressive moving average process

Definition 2.11 *$\{W_t\}$ is an autoregressive moving average process of order (p, q) (denoted by $ARMA(p, q)$) if it satisfies*

$$W_t - \phi_1 W_{t-1} - \cdots - \phi_p W_{t-p} = Z_t - \theta_1 Z_{t-1} - \cdots - \theta_q Z_{t-q}$$

where $\phi_1, \ldots, \phi_p$ and $\theta_1, \ldots, \theta_q$ are constants and $\{Z_t\}$ is a purely random process.

Equivalently, the model may be written in the form

$$\phi(B)W_t = \theta(B)Z_t$$

where

$$\phi(B) = 1 - \phi_1 B - \cdots - \phi_p B^p,$$

$$\theta(B) = 1 - \theta_1 B - \cdots - \theta_q B^q$$

and the conditions for stationarity and invertibility of the process are zeroes of the characteristic equations $\phi(B) = 0$ and $\theta(B) = 0$ lie outside the unit circle.

Uniqueness of Autoregressive Moving Average Model

With the assumption of Normality, knowledge of the first and second moments of the probability distribution implies complete knowledge of the distribution. In particular, knowledge of the mean and its autocovariance function can uniquely determine the probability structure of the model. Although this unique probability structure can

be represented by a multiplicity of linear models, nevertheless, uniqueness is achieved in the model when the appropriate stationarity and invertibility restrictions are introduced [4].

Suppose that $\{W_t\}$, with covariance generating function $\gamma(B)$, is represented by the linear model

$$\phi(B)W_t = \theta(B)Z_t \tag{2.2}$$

where zeroes of $\phi(B)$ and $\theta(B)$ lie outside the unit circle. Then this linear model may also be written as

$$\prod_{i=1}^{p}(1 - G_iB)W_t = \prod_{j=1}^{q}(1 - H_jB)Z_t$$

where the G_i^{-1} are the zeroes of $\phi(B) = 0$ and H_j^{-1} are the zeroes of $\theta(B) = 0$, and both G_i, H_j lie inside the unit circle. Using the equation (2.1)

$$\begin{aligned}\gamma(B) &= \sigma_Z^2\psi(B)\psi(B^{-1}) \\ &= \sigma_Z^2\psi(B)\psi(F).\end{aligned}$$

The covariance generating function for $\{W_t\}$ is

$$\gamma(B) = \prod_{i=1}^{p}(1 - G_iB)^{-1}(1 - G_iF)^{-1}\prod_{j=1}^{q}(1 - H_jB)(1 - H_jF)\sigma_Z^2.$$

Since

$$(1 - H_jB)(1 - H_jF) = H_j^2(1 - H_j^{-1}B)(1 - H_j^{-1}F),$$

it follows that any one of the stochastic models

$$\prod_{i=1}^{p}(1 - G_iB)W_t = \prod_{j=1}^{q}(1 - H_j^{\pm 1}B)kZ_t$$

can have the same covariance generating function, if the constant k is appropriately chosen. If a real root H is inside the unit circle, H^{-1} will lie outside, or if a complex pair, say H_1 and H_2, are inside, then the pair H_1^{-1} and H_2^{-1} will lie outside. It follows that there will be only one stationary invertible model of the form (2.2) which has a given autocovariance function.

2.2.2 Circular Model

In this thesis we only consider boundaries which are simple closed curves.

Definition 2.12 *A curve is a simple closed curve if and only if the initial point and the terminal point coincide and the curve does not intersect itself.*

Since the contour is closed, the observed boundary points satisfy circular condition :

$$W_{u(N+t)} = W_{ut}, \qquad t = 1, \ldots, N, \qquad u = x, y$$

where $W_{ut} = \{W_{xt}, W_{yt}\}$, $\{W_{xt}\}$ and $\{W_{yt}\}$ are the X and Y coordinates of the boundary points.

The time series, $\{W_{ut}\}, u = x, y$, is fitted to a particular circular autoregressive moving average model of order (p, q) as follows

$$\phi_u(B) W_{ut} = \theta_u(B) Z_{ut}, \qquad t = 1, \ldots, N, \qquad u = x, y$$

where

$$\begin{aligned} \phi_u(B) &= 1 - \phi_{u1} B - \cdots - \phi_{up} B^p, \\ \theta_u(B) &= 1 - \theta_{u1} B - \cdots - \theta_{uq} B^q \end{aligned}$$

and

$$Z_{u(N+t)} = Z_{ut}$$

where $\{Z_{ut}\}$ is independent, identical $N(0, \sigma^2_{Z_u})$ and the parameters $\phi_{u1}, \ldots, \phi_{up}$, $\theta_{u1}, \ldots, \theta_{uq}$, $\sigma^2_{Z_u}$ are unknown for $u = x, y$.

The procedures for estimating the unknown parameters of the time series $\{W_{xt}\}$ and $\{W_{yt}\}$ of order (p, q) are the same, therefore, we consider the following circular model:

$$\phi(B)W_t = \theta(B)Z_t, \qquad t = 1, \ldots, N$$

where

$$W_{N+t} = W_t, \qquad Z_{N+t} = Z_t,$$

$$\begin{aligned} \phi(B) &= 1 - \phi_1 B - \cdots - \phi_p B^p, \\ \theta(B) &= 1 - \theta_1 B - \cdots - \theta_q B^q \end{aligned}$$

and $\{Z_t\}$ are independent identical $N(0, \sigma_Z^2)$.

Let us assume that the process is stationary. The parameters $\theta_1, \ldots, \theta_q$ are chosen so that the roots of the equation $\theta(B) = 0$ lie outside the unit circle, implying that the model is both stationary and invertible. It is also assumed that no zeroes lie on the unit circle. The method of maximum likelihood and AIC, Akaike's Information Criterion [2], [6], [39], are used to estimate the parameters and the order of the model respectively.

Chapter 3

Estimation of Parameters

The method to estimate the unknown parameters of the circular model from Chapter 2 will be discussed. The estimation procedure is divided into two stages. First, we find the initial values for the CARMA parameter estimates and then we use these initial values to estimate the parameters iteratively.

3.1 Estimation of Mean, Variance and Autocovariance of the Time Series

In practice, a finite number of observations of the time series, $w_1, \ldots, w_N$, is provided from which the mean, variance and autocovariance are estimated. The mean, μ, of the process is zero and the variance, ${\sigma_W}^2$, of the process is estimated by

$$\hat{\sigma}_W^2 = \frac{1}{N}\sum_{t=1}^{N} w_t^2.$$

The autocovariance at lag k is estimated by

$$\hat{\gamma}_k = \frac{1}{N}\sum_{t=1}^{N} w_t w_{t+k} \tag{3.1}$$

where $k = 0, 1, \ldots, K$ and $K < N$.

The parameters of the model are estimated for different orders and the corresponding AIC values are calculated by using these estimates. The appropriate order of the model is determined by the values of p and q at which AIC attains its minimun.

3.2 Initial Estimation

The calculation of the initial values for the CARMA (p, q) parameter estimates is based on the first $(p+q+1)$ autocovariance $\hat{\gamma}_j, j = 0, 1, \ldots, p+q$ of W_t and proceeds in two stages [4].

3.2.1 Stage 1. Estimation of Autoregressive Parameters

The model is in the form

$$\phi(B)W_t = \theta(B)Z_t$$

which can be written as

$$W_t = \phi_1 W_{t-1} + \cdots + \phi_p W_{t-p} + Z_t - \theta_1 Z_{t-1} - \cdots - \theta_q Z_{t-q}. \tag{3.2}$$

On multiplying throughout equation (3.2) by W_{t-k} and taking expectation, it follows that

$$\begin{aligned} \gamma_k &= \phi_1\gamma_{k-1} + \cdots + \phi_p\gamma_{k-p} + \\ &\quad \gamma_{wz}(k) - \theta_1\gamma_{wz}(k-1) - \cdots - \theta_q\gamma_{wz}(k-q) \end{aligned} \tag{3.3}$$

where $\gamma_{wz}(k)$ is the cross covariance function between W_{t-k} and Z_t, defined below

$$\gamma_{wz}(k) = E[W_{t-k}Z_t].$$

Since W_{t-k} depends only on the Z_t's which have occured up to time $t-k$, it follows that

$$\begin{aligned} \gamma_{wz}(k) &= 0 \quad \text{for} \quad k > 0, \\ \gamma_{wz}(k) &\neq 0 \quad \text{for} \quad k \leq 0. \end{aligned}$$

Therefore, from equation (3.3), we have

$$\gamma_k = \phi_1\gamma_{k-1} + \cdots + \phi_p\gamma_{k-p}, \qquad N > k \geq q+1. \tag{3.4}$$

Using the above equation (3.4), initial values for the autoregressive parameters $\phi_1, \ldots, \phi_p$ can be obtained by solving the following system of linear equations

$$\hat{\gamma}_{q+1} = \hat{\phi}_1\hat{\gamma}_q + \hat{\phi}_2\hat{\gamma}_{q-1} + \cdots + \hat{\phi}_p\hat{\gamma}_{q-p+1},$$

$$\begin{aligned}
\hat{\gamma}_{q+2} &= \hat{\phi}_1\hat{\gamma}_{q+1} + \hat{\phi}_2\hat{\gamma}_q + \cdots + \hat{\phi}_p\hat{\gamma}_{q-p+2}, \\
&\vdots \\
\hat{\gamma}_{q+p} &= \hat{\phi}_1\hat{\gamma}_{q+p-1} + \hat{\phi}_2\hat{\gamma}_{q+p-2} + \cdots + \hat{\phi}_p\hat{\gamma}_q,
\end{aligned}$$

where the estimates of γ_k are given in equation (3 1).

3.2.2 Stage 2. Estimation of Moving Average Parameters

Let $W_t' = \phi(B)W_t$, the process can be written in the form of moving average process

$$W_t' = \theta(B)Z_t. \tag{3.5}$$

Expressing the autocovariance γ_k' of W_t' in terms of the autocovariance γ_k and ϕ_i's, we have

$$\begin{aligned}
E[W_{t-k}'W_t'] &= E[\phi(B)W_{t-k}\phi(B)W_t] \\
&= E[(W_{t-k} - \phi_1 W_{t-k-1} \cdots - \phi_p W_{t-k-p}) \\
&\qquad (W_t - \phi_1 W_{t-1} - \cdots - \phi_p W_{t-p})].
\end{aligned}$$

Consider the terms with autocovariances γ_{k+i} and γ_{k-i}. We have

$$\gamma_k' = \gamma_k \sum_{i=0}^{p} \phi_i^2 + \alpha_k \sum_{i=1}^{p} (\phi_0\phi_i + \phi_1\phi_{i+1} + \cdots + \phi_{p-i}\phi_p)$$

where

$$\begin{aligned}
k &= 0, 1, \ldots, q, \\
\alpha_k &= \gamma_{k+i} + \gamma_{k-i}, \\
\phi_0 &= -1.
\end{aligned}$$

Therefore, the estimates of the autocovariance of $W_t' = \theta(B)Z_t$ are

$$\hat{\gamma}_k' = \hat{\gamma}_k \sum_{i=0}^{p} \hat{\phi}_i^2 + \hat{\alpha}_k \sum_{i=1}^{p} (\hat{\phi}_0\hat{\phi}_1 + \hat{\phi}_1\hat{\phi}_{i+1} + \cdots + \hat{\phi}_{p-i}\hat{\phi}_p)$$

where

$$\begin{aligned}
k &= 0, 1, \ldots, q, \\
\hat{\alpha}_k &= \hat{\gamma}_{k+i} + \hat{\gamma}_{k-i}, \\
\phi_0 &= -1;
\end{aligned}$$

which is equivalent to

$$\hat{\gamma}'_k = \begin{cases} \sum_{i=0}^{p} \sum_{j=0}^{p} \hat{\phi}_{i0}\hat{\phi}_{j0}\hat{\gamma}_{|k+i-j|} & \text{for } p > 0 \quad (\hat{\phi}_{00} = -1), \\ \hat{\gamma}_k & \text{for } p = 0. \end{cases}$$

Using the autocovariance estimates $\hat{\gamma}'_k$ from above, the initial values for the moving average parameters in equation (3.5) can be obtained by the following.

Consider the moving average process, $W'_t = \theta(B)Z_t$. The autocovariance function at lag k is

$$\begin{aligned} \gamma'_k &= E[(Z_t - \theta_1 Z_{t-1} - \cdots - \theta_q Z_{t-q}) \\ &\qquad (Z_{t-k} - \theta_1 Z_{t-k-1} - \cdots - \theta_q Z_{t-k-q})]. \end{aligned}$$

Hence, the variance of the process is

$$\gamma'_0 = (1 + \theta_1^2 + \cdots + \theta_q^2)\sigma_Z^2$$

and

$$\gamma'_k = \begin{cases} (-\theta_k + \theta_1\theta_{k+1} + \cdots + \theta_{q-k}\theta_q)\sigma_Z^2 & \text{for } k = 1, \ldots, q, \\ 0 & \text{for } k > q. \end{cases}$$

Substituting $\gamma'_0, \gamma'_1, \ldots, \gamma'_q$ by the corresponding estimates $\hat{\gamma}'_0, \hat{\gamma}'_1, \ldots, \hat{\gamma}'_q$ the following equations are obtained

$$\hat{\sigma}_Z^2 - \frac{\hat{\gamma}'_0}{1 + \hat{\theta}_1^2 + \cdots + \hat{\theta}_q^2} = 0, \tag{3.6}$$

$$\hat{\theta}_k + \frac{\hat{\gamma}'_k}{\hat{\sigma}_Z^2} - \hat{\theta}_1\hat{\theta}_{k+1} - \hat{\theta}_2\hat{\theta}_{k+2} - \cdots - \hat{\theta}_{q-k}\hat{\theta}_q = 0 \quad \text{for } k = 0, 1, \ldots, q.$$

The initial values of the parameters, $\hat{\theta}_{10}, \ldots, \hat{\theta}_{q0}$, are obtained by solving the above set of nonlinear equations with $\hat{\theta}_{10} = \cdots = \hat{\theta}_{q0} = 0$ as starting values by using the Newton Raphson method [38], see Appendix A1. Unlike the corresponding autoregressive estimates, the resulting estimates may not have high statistical efficiency. However, they can provide useful starting values for an iterative procedure discussed in the next section and they will converge to the maximum likelihood estimates.

Once the initial estimates of parameters $\hat{\theta}_{10}, \ldots, \hat{\theta}_{q0}$ are calculated, these values are substituted into the equation

$$1 + \hat{\theta}_{10}B + \cdots + \hat{\theta}_{q0}B^q = 0$$

which is solved by the Laguerre's method [38], see Appendix A2. Any of the real or complex roots that lie inside the unit circle, are replaced by their reciprocals and then the new values of $\hat{\theta}_{i0}, i = 1, \ldots, q$ are calculated. All the roots should lie outside the unit circle because there is only one stationary invertible model corresponding to a given autocovariance function.

3.2.3 Estimation of the Residual Variance

The variance of the residuals is estimated by the following formulas

$$\hat{\sigma}_Z^2 = \begin{cases} \hat{\gamma}_0 - \sum_{i=1}^{p} \hat{\phi}_i \hat{\gamma}_i & \text{for } q = 0, \\ \hat{\sigma}_Z^2 & \text{for } q > 0 \text{ from equation (3.6).} \end{cases}$$

Indeed, when $q = 0$, we have

$$W_t = \phi_1 W_{t-1} + \cdots + \phi_p W_{t-p} + Z_t.$$

On multiplying throughout by W_t and taking expection, we obtain

$$\gamma_0 = \phi_1 \gamma_{-1} + \cdots + \phi_p \gamma_{-p} + \sigma_Z^2.$$

Since $\gamma_i = \gamma_{-i}$ that implies we have the estimate

$$\hat{\sigma}_Z^2 = \hat{\gamma}_0 - \sum_{i=0}^{p} \hat{\phi}_i \hat{\gamma}_i.$$

3.3 Model Estimation

One way to estimate the parameters of the model is the method of maximum likelihood. This method usually produces good estimates but is time consuming. In most situations, the maximum likelihood estimates are closely approximated by the least squares estimates, which are easier to obtain. In our application, both methods produce the same estimates.

3.3.1 Maximum Likelihood Function of the Model

The circular model of order (p, q) with N observations $w_1, \ldots, w_N$, is represented by

$$\phi(B) W_t = \theta(B) Z_t, \qquad t = 1, \ldots, N,$$

where

$$W_{N+t} = W_t, \qquad Z_{N+t} = Z_t,$$

$$\begin{aligned} \phi(B) &= 1 - \phi_1 B - \ldots - \phi_p B^p, \\ \theta(B) &= 1 - \theta_1 B - \ldots - \theta_q B^q, \end{aligned}$$

the mean is zero and the Z_t's are independent identical $N(0, \sigma_Z^2)$.

Since the model is stationary and invertible, therefore the model can be written in the form

$$\begin{aligned} Z_t &= \theta^{-1}(B)\phi(B)W_t \\ &\simeq W_t - \psi_1 W_{t-1} - \cdots - \psi_h W_{t-h} \end{aligned}$$

where the ψ's are functions of ϕ's and θ's. The last equality is only approximate since infinite series is replaced by a finite truncation at the term $h+1$. The value of $h, 0 \leq h \leq N$, is chosen so that the autocorrelation, $\rho(h)$, between W_t and W_{t-h} is negligible. Substituting the observations $\boldsymbol{W} = (w_1, \ldots, w_N)$ into the above equation, we have

$$\begin{aligned} z_1 &= w_1 - \psi_1 w_0 - \cdots - \psi_h w_{1-h}, \\ z_2 &= w_2 - \psi_1 w_1 - \cdots - \psi_h w_{2-h}, \\ &\vdots \\ z_N &= w_N - \psi_1 w_{N-1} - \cdots - \psi_h w_{N-h}, \end{aligned}$$

where $\boldsymbol{W}_* = (w_{1-h}, \ldots, w_0)$ are observations before the commencement of the series. Since the Z_t's are $N(0, \sigma_Z^2)$, so the joint conditional probability density function of z_t's given $w_{1-h}, \ldots, w_0$ is

$$p(\boldsymbol{Z}|\boldsymbol{W}_*) = \left(\frac{1}{2\pi\sigma_Z{}^2}\right)^{\frac{N}{2}} \exp\left\{-\frac{\boldsymbol{Z}^t\boldsymbol{Z}}{2\sigma_Z{}^2}\right\}$$

where $\boldsymbol{Z}^t$ is the vector $(z_1, \ldots, z_N)$ and $\boldsymbol{Z}^t$ is the transpose of $\boldsymbol{Z}$. It is easily seen that the transformation has unit Jacobian, therefore the joint conditional probability density function of $w_1, \ldots, w_N$ given $w_{1-p}, \ldots, w_0$ is

$$p(\boldsymbol{W}|\boldsymbol{W}_*) = \left(\frac{1}{2\pi\sigma_Z{}^2}\right)^{\frac{N}{2}} \exp\left\{-\frac{S(\psi)}{2\sigma_Z{}^2}\right\}$$

where

$$S(\psi) = \sum_{t=1}^{N} (w_t - \psi_1 w_{t-1} - \cdots - \psi_h w_{t-h})^2$$

and ψ is the vector $(\psi_1, \ldots, \psi_h)$. The log likelihood function is

$$\ln L(\psi, \sigma_Z) = -\frac{N}{2} \ln(2\pi {\sigma_Z}^2) - \frac{S(\psi)}{2{\sigma_Z}^2}.$$

The observations, $\boldsymbol{W}_*$, before the commencement of the series can be obtained by the relationship $W_{N+t} = W_t$. Since

$$\begin{aligned} z_t &= w_t - \psi_1 w_{t-1} - \cdots - \psi_h w_{t-h} \\ &\simeq w_t - \phi_1 w_{t-1} - \cdots - \phi_p w_{t-p} + \theta_1 z_{t-1} + \cdots + \theta_q z_{t-q}, \end{aligned}$$

therefore

$$\begin{aligned} S(\psi) &\simeq S(\phi, \theta) \\ &= \sum_{t=1}^{N} (w_t - \phi_1 w_{t-1} - \cdots - \phi_p w_{t-p} + \theta_1 z_{t-1} + \cdots + \theta_q z_{t-q})^2. \end{aligned}$$

With the knowledge of $\phi, \theta, \boldsymbol{W}$ and by the circularity, the residuals can be calculated by solving the set of equations which will be discussed in next section. In order to estimate the parameters, the log likelihood function is maximized or $S(\phi, \theta)$ is miminized resulting in the least squares estimates of parameters.

Residuals

Once the parameters are estimated, the residuals can be calculated by solving the system of linear equations

$$\begin{bmatrix} 1 & 0 & 0 & \cdots & 0 & 0 & -\hat{\phi}_p & -\hat{\phi}_{p-1} & \cdots & -\hat{\phi}_1 \\ -\hat{\phi}_1 & 1 & 0 & \cdots & 0 & 0 & 0 & -\hat{\phi}_p & \cdots & -\hat{\phi}_2 \\ & & & & & & \vdots & & & \\ 0 & 0 & 0 & \cdots 0 & 0 & -\hat{\phi}_p & -\hat{\phi}_{p-1} & -\hat{\phi}_{p-2} & \cdots & 1 \end{bmatrix} \begin{bmatrix} w_1 \\ w_2 \\ \vdots \\ w_N \end{bmatrix} =$$

$$\begin{bmatrix} 1 & 0 & 0 & \cdots & 0 & 0 & -\hat{\theta}_q & -\hat{\theta}_{q-1} & \cdots & -\hat{\theta}_1 \\ -\hat{\theta}_1 & 1 & 0 & \cdots & 0 & 0 & 0 & -\hat{\theta}_q & \cdots & -\hat{\theta}_2 \\ & & & & & & \vdots & & & \\ 0 & 0 & 0 & \cdots & 0 & -\hat{\theta}_q & -\hat{\theta}_{q-1} & -\hat{\theta}_{q-2} & \cdots & 1 \end{bmatrix} \begin{bmatrix} z_1 \\ z_2 \\ \vdots \\ z_N \end{bmatrix}$$

which can be rewritten as

$$\boldsymbol{A}\boldsymbol{w} = \boldsymbol{B}\boldsymbol{z}$$

where $\boldsymbol{A}, \boldsymbol{B}$ are the $N \times N$ matrices and $\boldsymbol{w}, \boldsymbol{z}$ are $N \times 1$ matrices. Thus, for any given set of parameters and observations, the residuals can be calculated.

3.3.2 Linearization of the Model

Since the model contains the moving average part, z_t is nonlinear function of the parameters. As a result, iterative approach of the least squares method is used to estimate the parameters of the circular model so that the sum

$$\sum_{t=1}^{N} {z_t}^2$$

is miminium.

Expanding z_t into Taylor series about its value corresponding to the set of initial values of the parameters, $\boldsymbol{\zeta}_o(\zeta_{10}, \ldots, \zeta_{k0}), k = p + q$, where $\boldsymbol{\zeta} = (\boldsymbol{\phi}, \boldsymbol{\theta})$ and ignoring terms of order $\delta\boldsymbol{\zeta}^2$ and higher, it follows that

$$z_t = z_{t0} - \sum_{i=1}^{k} (\zeta_i - \zeta_{i0}) x_{it} \tag{3.7}$$

where

$$x_{it} = -\left.\frac{\partial z_t}{\partial \zeta_i}\right|_{\boldsymbol{\zeta}=\boldsymbol{\zeta}_o}.$$

Now if $\boldsymbol{X}$ is the $N \times k$ matrix $\{x_{it}\}$, N equations of the form (3.7) are combined into the system

$$\boldsymbol{z}_o = \boldsymbol{X}(\boldsymbol{\zeta} - \boldsymbol{\zeta}_o) + \boldsymbol{z}$$

where $\boldsymbol{z}_o$ and $\boldsymbol{z}$ are column vectors with N elements. The partial derivative can be calculated numerically by using the method from Appendix A1. The adjustment $\boldsymbol{\zeta} - \boldsymbol{\zeta}_o$, can be obtained by the method of linear least squares

$$\delta\boldsymbol{\zeta} = \boldsymbol{\zeta} - \boldsymbol{\zeta}_o = (\boldsymbol{X}^t\boldsymbol{X})^{-1}\,\boldsymbol{X}^t\boldsymbol{z}_o$$

where $\boldsymbol{X}^t$ is the transpose of the matrix $\boldsymbol{X}$ and $(\boldsymbol{X}^t\boldsymbol{X})^{-1}$ is the inverse of the matrix $(\boldsymbol{X}^t\boldsymbol{X})$.

Since the z_t's are not linear in the parameters $\boldsymbol{\zeta}$, a single adjustment will not immediately produce the least squares values. Instead, the adjusted values are substituted as new values and the process is iterated until $S(\boldsymbol{\phi}, \boldsymbol{\theta})$ reaches minimum. Convergence is assumed if $S(\boldsymbol{\zeta}^{new}) < S(\boldsymbol{\zeta}^{old})$ and $|\zeta_i^{new} - \zeta_i^{old}| < \varepsilon$ for $i = 1, \ldots, p+q$, or a specific number of iterations, k, has been taken. When divergence occurs, the set of parameters is chosen as the best result in the first k iterations.

3.3.3 Estimation of the Residual Variance

The log likelihood function is

$$\begin{aligned} \ln L(\boldsymbol{\psi}, \sigma_Z) &= \ln L(\boldsymbol{\phi}, \boldsymbol{\theta}, \sigma_Z) \\ &= \text{const} - \frac{N}{2} \ln \sigma_Z^2 - \frac{S(\boldsymbol{\phi}, \boldsymbol{\theta})}{2\sigma_Z^2}. \end{aligned}$$

Taking partial derivative of the above equation with respect to σ_Z, and equating it to zero, the estimate of the variance is

$$\hat{\sigma}_Z^2 = \frac{S(\boldsymbol{\phi}, \boldsymbol{\theta})}{N}.$$

3.3.4 Order of the Model

In the preceding section, the problem of parameter estimation is discussed under the assumption that the orders of the autoregressive and moving average parts are known. In practice, these orders are unknown. A criterion to determine the order of the model will be described below.

The order of the model is determined by the AIC, Akaike's Information Criterion [2], [6], [39], which can be used for a statistical model identification in a wide range of situations and is not restricted to the time series context. The AIC is defined as follows

Definition 3.1

$$AIC(p, q) = -2 \ln[\textit{maximum likelihood}] + 2(p + q).$$

From the previous section, it is shown that when the log likelihood function is maximized with respect to ϕ and θ, the estimate of the variance is given by

$$\hat{\sigma}_Z^2 = \frac{S(\phi, \theta)}{N}.$$

Subsitiuting the above into the log likelihood function and omitting the terms which are independent of ϕ, θ, p and q, the AIC criterion becomes

$$\mathrm{AIC}(p, q) = N \ln \hat{\sigma}_Z^2 + 2(p + q).$$

The appropriate order of the model is determined by the value of p and q at which $\mathrm{AIC}(p, q)$ attains its minimum.

Chapter 4

Properties and Reconstruction

In this chapter, the properties of the parameters and their estimates will be discussed. The reconstruction of the closed curves using different numbers of quantization levels of residuals and the results of simulation are presented.

4.1 Invariance

It is customary to regard the shape of a boundary as invariant to translations, rotations and scaling of the boundary. As a result, more than one set of sequences $\{W_{ut}\}, u = x, y$, would correspond to the same shape. The following specifies the conditions under which the sequences $\{W_{ut}\}$ and $\{W_{ut'}\}$ correspond to the same shape.

Definition 4.1 *Consider two circular boundary sequences* $\{W_{ut}\}$ *and* $\{W_{ut'}\}$, $u = x, y$. *The boundaries corresponding to* $\{W_{ut}\}$ *and* $\{W_{ut'}\}$ *have the same shape if the following condition is satisfied*

$$W_{ut'} = bW_{u(t+c)}, \qquad u = x, y$$

where $b > 0, c$ *is an integer and* $|c| \leq N - 1$ *for all integers* t.

When $c = 0$, the sequence $\{W_{ut'}\}, u = x, y$, is obtained from $\{W_u\}$ by scaling. When $b = 1$ and c is a nonzero integer, the boundary represented by $\{W_{ut'}\}$ is a rotated version of the boundary $\{W_{ut}\}$ or equivalently $\{W_{ut'}\}$ and $\{W_{ut}\}$ are obtained from the same boundary but with different starting points. The coordinates of the

boundary points, are obtained relative to the centroid of the boundary, therefore the sequences $\{W_{ut}\}$ are invariant to translation of the boundary. The relationship between the parameters of different sequences which correspond to identical shapes, is given in the following theorem

Theorem 4.1 *Consider two circular boundary sequences of order* (p,q) : $\{W_{ut}\}$, $u = x,y$, *such that* $\phi_u(B)W_{ut} = \theta_u(B)Z_{ut}$ *and* $\{W_{ut'}\}, u = x,y$, *such that* $\phi'_u(B)W'_{ut} = \theta'_u(B)Z'_{ut}$, *where* $\{Z_{ut}\}$ *and* $\{Z'_{ut}\}$ *are independent identical* $N(0,\sigma^2_{Zu})$ *and* $N(0,\sigma^2_{Z'u})$ *respectively and*

$$\begin{aligned}
\phi_u(B) &= 1 - \phi_{u1}B - \ldots - \phi_{up}B^p, \\
\theta_u(B) &= 1 - \theta_{u1}B - \ldots - \theta_{uq}B^q, \\
\phi'_u(B) &= 1 - \phi'_{u1}B - \ldots - \phi'_{up}B^p, \\
\theta'_u(B) &= 1 - \theta'_{u1}B - \ldots - \theta'_{uq}B^q.
\end{aligned}$$

Let $\boldsymbol{\phi}'_u$ *be* $(\phi'_{u1},\ldots,\phi'_{up})$, $\boldsymbol{\phi}_u$ *be* $(\phi_{u1},\ldots,\phi_{up})$, $\boldsymbol{\theta}'_u$ *be* $(\theta'_{u1},\ldots,\theta'_{uq})$ *and* $\boldsymbol{\theta}_u$ *be* $(\theta_{u1},\ldots,\theta_{uq})$. $\{W'_{ut}\}$ *and* $\{W_{ut}\}$ *have the same shape if* $\boldsymbol{\phi}'_u = \boldsymbol{\phi}_u$, $\boldsymbol{\theta}'_u = \boldsymbol{\theta}_u$ *and* $Z'_{ut} = kZ_{u(l+t)}$ *where* k *is a positive real number and* l *and* t *are integers.*

Proof Without loss of generality, identity of the shape is obtained by showing

$$W'_{ut} = kW_{ut} \quad \text{for} \quad k > 0$$

and

$$W'_{ut} = W_{u(t+l)} \quad \text{for} \quad |l| \leq N$$

where $u = x,y$.

The model is stationary and invertible, therefore

$$\begin{aligned}
\phi'_u(B)W'_{ut} &= \theta'_u(B)Z'_{ut} \\
\text{i.e.} \qquad W'_{ut} &= \phi_u^{-1}(B)\theta_u(B)kZ_{u(t+l)}.
\end{aligned}$$

Choosing $k = b, l = 0$, we have

$$\begin{aligned}
W'_{ut} &= b\phi_u^{-1}(B)\theta_u(B)Z_{ut} \\
&= bW_{ut},
\end{aligned}$$

choosing $k = 1, l = c$, we have

$$\begin{aligned} W'_{ut} &= \phi_u^{-1}(B)\theta_u(B)Z_{u(t+l)} \\ &= W_{u(t+l)}. \end{aligned}$$

This ends the proof.

The significance of this theorem lies in the following. Suppose $(\phi_u, \theta_u), u = x, y$, corresponds to a boundary P and $(\phi'_u, \theta'_u), u = x, y$, corresponds to another boundary Q, where Q is obtained from P by scaling, translation and variation in the starting point. Then $\phi_u = \phi'_u$ and $\theta_u = \theta'_u$, i.e. given two identical closed shapes, the corresponding values of ϕ_u and θ_u are the same. This suggests the use of the vector ϕ_u and θ_u for classification purposes.

We obtained three types of invariance for the vector ϕ_u and θ_u, $u = x, y$ as follows

1. invariance to scaling of the boundary,
2. invariance to variation of the starting point,
3. invariance to translation of the boundary.

An effective normalization is done with respect to the center of gravity of the shape, so that ϕ_u and θ_u, $u = x, y$, obey property 3.

Theorem 4.2 *Let $(\hat{\phi}_u, \hat{\theta}_u), u = x, y$, denote the estimates of the parameters of the circular model $\phi_u(B)W_{ut} = \theta_u(B)Z_{ut}, t = 1, \ldots, N$. Then $(\hat{\phi}_u, \hat{\theta}_u)$ satisfy the properties 1 and 2.*

The estimates of parameters are also invariant to translations because the boundary sequences are obtained relative to the centroid. The proof is similiar to the proof of theorem 4.1 and is omitted.

4.2 Reconstruction

The boundary sequences are represented by the model $\phi_u(B)W_{ut} = \theta_u(B)Z_{ut}$, $t = 1, \ldots, N, u = x, y$, where W_{ut} is the observation at time t and Z_{ut} is the corresponding residual. The information contained in the original correlated observations

is split in the model into two sets, the statistical information contained in the set $\boldsymbol{\phi}_u$, $\boldsymbol{\theta}_u$ and the information in the uncorrelated residuals $\{z_{ut}\}$. A curve identical to the original one will be obtained if the original sets of residuals are used to reconstruct the curve. Quantized residuals [17], [31], $\{\hat{z}_{ut}\}$, are used to reconstruct the closed curve to test the statistical information contained in the vectors $\hat{\boldsymbol{\phi}}_u$ and $\hat{\boldsymbol{\theta}}_u$. From the information of $\hat{\boldsymbol{\phi}}_u$ and $\hat{\boldsymbol{\theta}}_u$ and $\{\hat{z}_{ut}\}$, a boundary which is close to the original one can be obtained.

The boundary sequences, $\widehat{\boldsymbol{W}}_u, u = x, y$, can be obtained by minimizing the norm

$$||\boldsymbol{B}(\hat{\boldsymbol{\phi}}_u)\widehat{\boldsymbol{W}}_u - \boldsymbol{B}(\hat{\boldsymbol{\theta}}_u)\widehat{\boldsymbol{Z}}_u||^2,$$

where

$$\widehat{\boldsymbol{Z}}'_u = (\hat{z}_{u1}, \ldots, \hat{z}_{uN}), \qquad \widehat{\boldsymbol{W}}'_u = (\hat{w}_{u1}, \ldots, \hat{w}_{uN}),$$

$$\boldsymbol{B}(\hat{\boldsymbol{\phi}}_u) = \begin{bmatrix} 1 & 0 & 0 & \cdots & 0 & 0 & -\hat{\phi}_p & -\hat{\phi}_{p-1} & \cdots & -\hat{\phi}_1 \\ -\hat{\phi}_1 & 1 & 0 & \cdots & 0 & 0 & 0 & -\hat{\phi}_p & \cdots & -\hat{\phi}_2 \\ & & & & & & \vdots & & & \\ 0 & 0 & 0 & \cdots & 0 & -\hat{\phi}_p & -\hat{\phi}_{p-1} & -\hat{\phi}_{p-2} & \cdots & 1 \end{bmatrix},$$

$$\boldsymbol{B}(\hat{\boldsymbol{\theta}}_u) = \begin{bmatrix} 1 & 0 & 0 & \cdots & 0 & 0 & -\hat{\theta}_q & -\hat{\theta}_{q-1} & \cdots & -\hat{\theta}_1 \\ -\hat{\theta}_1 & 1 & 0 & \cdots & 0 & 0 & 0 & -\hat{\theta}_q & \cdots & -\hat{\theta}_2 \\ & & & & & & \vdots & & & \\ 0 & 0 & 0 & \cdots & 0 & -\hat{\theta}_q & -\hat{\theta}_{q-1} & -\hat{\theta}_{q-2} & \cdots & 1 \end{bmatrix}.$$

Different number of quantization levels are used for the reconstruction and the results are presented in next section.

4.3 Simulation

The experiments are performed on several digitized characters chosen from Suen's database [27] as shown in Figure 4.1 and denoted as characters '1','3','5' and '9'. The number of points obtained from the boundary is 100, the values for both p and q vary from 0 to 5 for both $\{W_{xt}\}$ and $\{W_{yt}\}$. For initial values and model estimation, the value of ε is 0.001, the value of δ for calculating the derivative numerically is 0.01 and the number of iteration, k, is 20. The value of AIC is calculated for each order (p, q)

and the optimal order is chosen as the minimum value of AIC. The exact residuals are quantized using the Max quantizer [31] assuming a Gaussian distribution for the residuals. The experiments were performed on Sun 3/50 workstation. Some of the AIC values and the corresponding orders are shown in tables 4.1 and 4.2 for $\{W_{xt}\}$ and $\{W_{yt}\}$ respectively.

Order	'1'	'3'	'5'	'9'
1, 1	−213.73	−59.00	−162.01	−155.19
2, 1	−373.35	−108.32	−241.49	−316.98
2, 4	−389.66	−111.00	−254.65	−313.12
2, 5	−388.89	−112.70	−246.11	−328.67
3, 2	−357.49	−103.63	−249.06	−300.72
4.0	−379.53	−106.55	−244.21	−324.14
4, 5	−342.16	−102.38	−242.57	−332.57
5, 1	−379.51	−101.43	−205.50	−271.30
Optimal Order	2, 4	2, 5	2, 4	4, 5

Table 4.1: AIC Values For Time Series $\{W_{xt}\}$.
For Characters '1', '3', '5' and '9'.

Order	'1'	'3'	'5'	'9'
1, 1	−280.35	15.21	−7.91	−210.62
2, 0	−330.72	−128.70	−272.28	−256.84
2, 1	−331.13	−127.52	−270.82	−256.39
2, 2	−346.45	−125.63	−269.12	−267.95
3, 2	−326.56	−122.84	−265.72	−266.07
4.0	−340.55	−125.56	−269.58	−268.60
4, 2	−331.29	−117.51	−267.29	−265.32
5, 2	−305.86	−125.76	−266.01	−263.32
Optimal Order	2, 2	2, 0	2, 0	4, 0

Table 4.2: AIC Values For Time Series $\{W_{yt}\}$.
For Characters '1', '3', '5' and '9'.

For the reconstruction, different levels of quantized resdiuals are used. Figure 4.2, Figure 4.3 and Figure 4.4 show the reconstructed characters by using quantized residuals with 36, 26 and 16 output levels with the corresponding optimal orders from the given tables. The reconstructions shown in Figure 4.2 are quite good for all the characters because most of the information is preserved during quantization. As the number of quantization levels decreases, the quality of reconstruction also decresases, see Figure 4.3 and Figure 4.4, but not substantially. It can be seen from these results that estimates of the parameters carry significant statistical information about the shapes because as the number of quantization levels decreases, the quality of the reconstructed characters remains good enough for recognition. This suggests that the parameters are good candidates for character recognition and classification.

Figure 4.5 shows the reconstructed characters using CARMA model of order $(2,1)$ for both $\{W_{xt}\}$ and $\{W_{yt}\}$ and Figure 4.6 shows the reconstructed characters using model of order $(3,2)$ for both $\{W_{xt}\}$ and $\{W_{yt}\}$. All of the characters are reconstructed by using quantized residuals with 16 output level. The reconstructed characters can still be recognized, implying that the reconstruction process is not very sensitive to the model order as long as that order does not differ much from the optimal order.

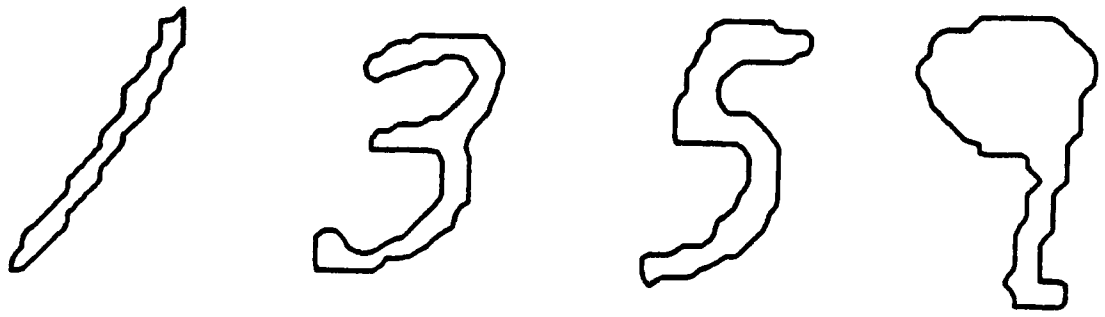

Figure 4.1: Original Shapes:Characters '1', '3', '5', and '9'.

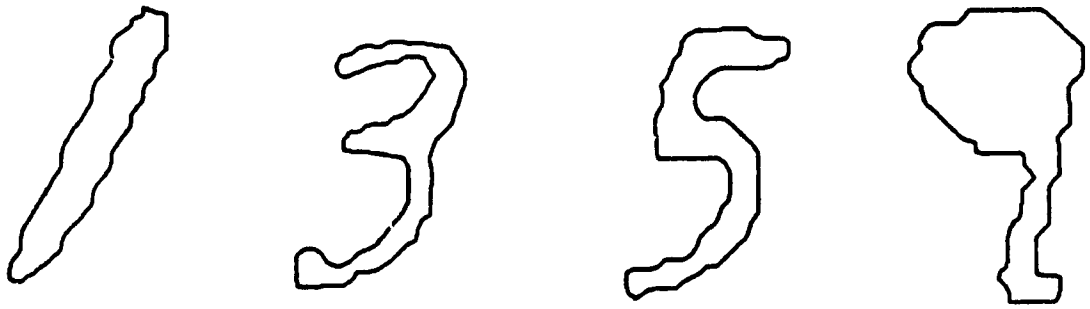

Figure 4.2: Reconstructed Shapes:Optimal order and 36 output quantization levels. Characters '1', '3', '5', and '9'.

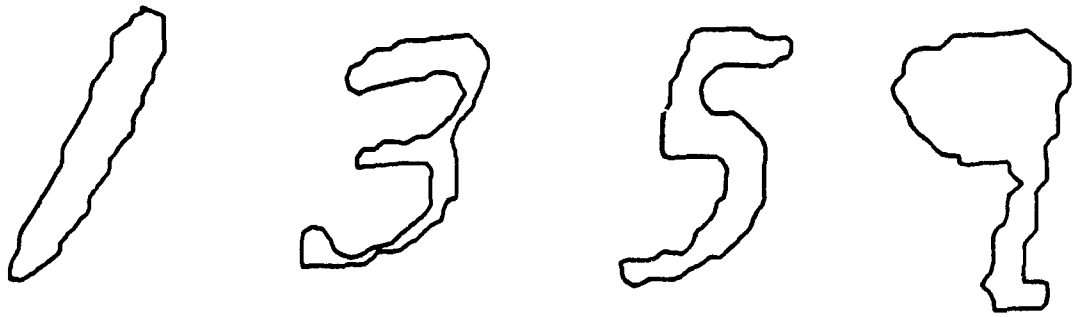

Figure 4.3: Reconstructed Shapes:Optimal order and 26 output quantization levels. Characters '1', '3', '5', and '9'.

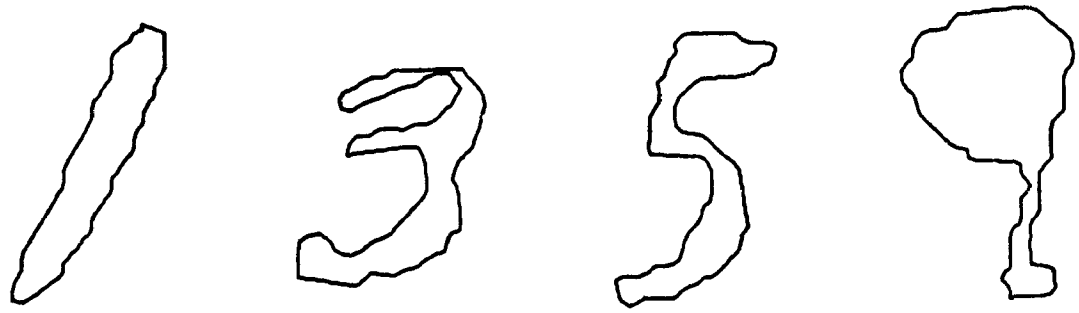

Figure 4.4: Reconstructed Shapes:Optimal order and 16 output quantization levels. Characters '1', '3', '5', and '9'.

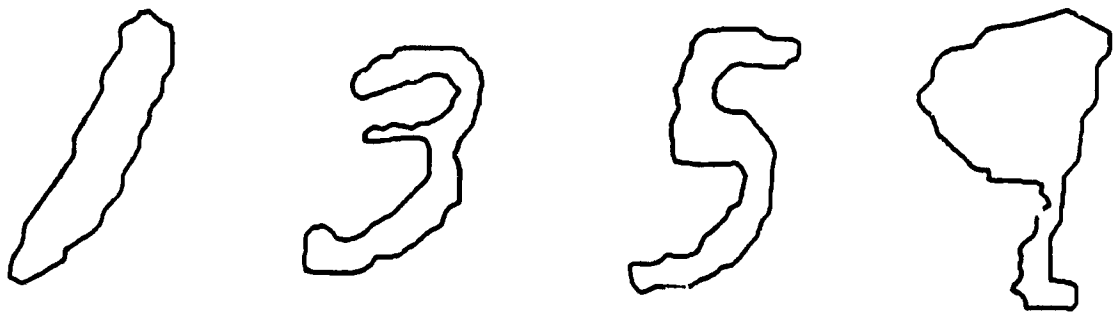

Figure 4.5: Reconstructed Shapes:Order (2,1) and 16 output quantization levels. Characters '1', '3', '5', and '9'.

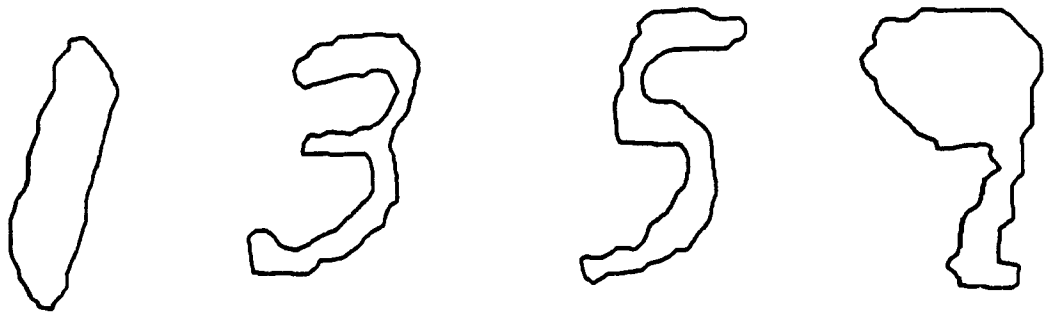

Figure 4.6: Reconstructed Shapes:Order (3,2) and 16 output quantization levels. Characters '1', '3', '5', and '9'.

Chapter 5

Fourier Series Approach

Another approach for coding the two dimensional pattern is the method of Fourier descriptors. The amplitudes of Fourier descriptors are shown to be invariant under rotations, translations, scaling, mirror reflections and shifts of the starting point.

5.1 Fourier Descriptors

Different kinds of Fourier descriptors for polygonal curves are obtained from different approaches, some examples are from Granlund [18], Persoon and Fu [37], Zahn and Roskies [45]. The Fourier descriptors defined in Zahn and Roskies [45], as well as their improvements and modifications will be discussed.

5.1.1 Linearized Step Signature

Zahn and Roskies [45] define Fourier descriptors of a curve as follows. Let γ be a clockwise oriented simple closed smooth curve of perimeter L with parametric representation $Z(l) = (x(l), y(l))$ where l is the arc length along the boundary from the chosen starting point, Z_0, and $0 \leq l \leq L$. Denote the angular direction of γ at point l by the function $\theta(l)$ and let $\delta_0 = \theta(0)$ be the absolute angular direction at the starting point Z_0. The cumulative angular bend function $\phi(l)$ is defined as the net amount of angular bend between starting point Z_0 and the point $Z(l)$ as shown in Figure 5.1a. So $\phi(l) = \theta(l) - \theta(0)$ except for possible multiples of 2π, $\phi(L) = -2\pi$ and $\phi(0) = 0$. The domain $[0, L]$ is normalized to the interval $[0, 2\pi]$ which is standard for periodic function.

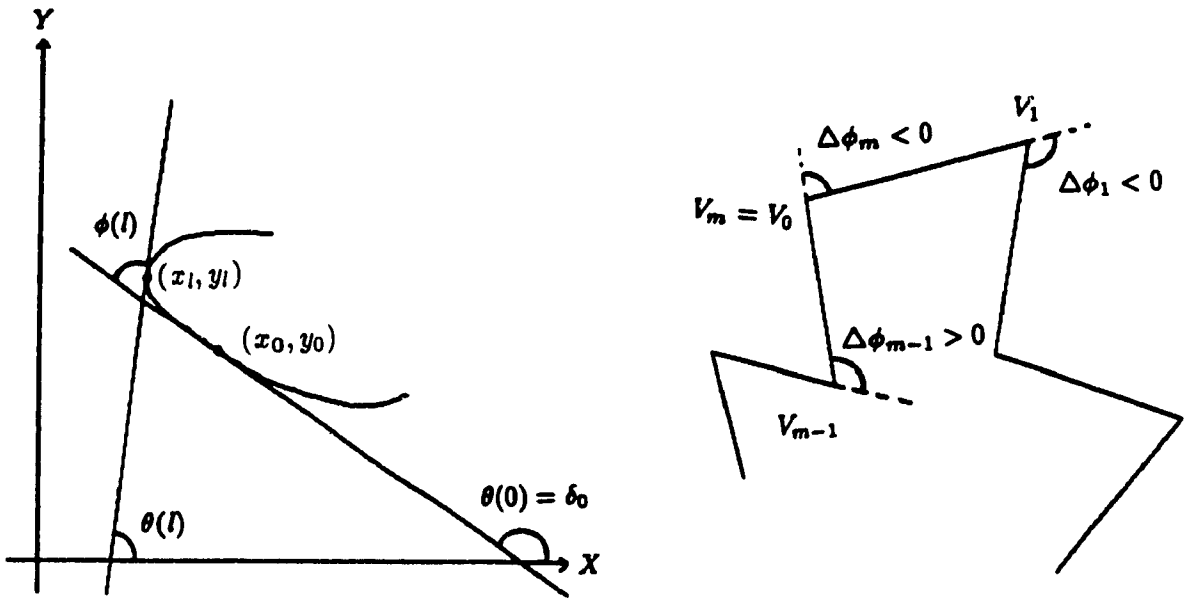

(a) Parametric representation of a plane curve with tangential direction $\theta(l)$ and cumulative angular bend $\phi(l)$.

(b) Description of a simple closed planar polygon in terms of edge lengths Δl_i and vertex bends $\Delta\phi_i$.

Figure 5.1: (a)Parametric representation.(b)Description of a simple closed polygon.

A linearized step signature is defined as

$$\phi^*(t) = \phi\left(\frac{Lt}{2\pi}\right) + t$$

and $\phi^*(t)$ is invariant under rotations, translations and scaling, making it a good candidate for shape signature. Expand ϕ^* as a Fourier series

$$\phi^*(t) = \mu_0 + \sum_{n=1}^{\infty}(a_n \cos nt + b_n \sin nt).$$

In polar form, the expansion is

$$\phi^*(t) = \mu_0 + \sum_{n=1}^{\infty} A_n \cos(nt - \alpha_n)$$

where (A_n, α_n) are polar coordinates of (a_n, b_n). The numbers A_n and α_n are the Fourier descriptors for the curve γ and are known as the nth harmonic amplitude and phase angle respectively.

Formulas for the Fourier coefficients, a_n, b_n, $n = 1, \ldots, N$, and μ_0 are derived when γ is a polygonal curve. Assuming that the curve, γ, has m vertices $V_0, \ldots, V_{m-1}$, $V_m = V_0$, and that the edge (V_{i-1}, V_i) has length Δl_i, $\Delta l_0 = 0$. The change in angular direction at vertex V_i is $\Delta\phi_i$ (negative in clockwise direction and positive in counter clockwise direction) and $L = \sum_{i=1}^{m} \Delta l_i$. With this definition (Figure 5.1b), it is not hard to verify that

$$\phi(l) = \sum_{i=1}^{k} \Delta\phi_i \qquad \text{for} \qquad \sum_{i=1}^{k} \Delta l_i \le l \le \sum_{i=1}^{k+1} \Delta l_i$$

and

$$\phi(0) = 0 \qquad \text{for} \qquad 0 \le l \le \Delta l_1.$$

Expanding ϕ^* in a Fourier series, we have

$$\phi^*(t) = \mu_0 + \sum_{n=1}^{\infty} (a_n \cos nt + b_n \sin nt)$$

where

$$\begin{aligned} \mu_0 &= \frac{1}{2\pi} \int_0^{2\pi} \phi^*(t) dt, \\ a_n &= \frac{1}{\pi} \int_0^{2\pi} \phi^*(t) \cos nt dt, \\ b_n &= \frac{1}{\pi} \int_0^{2\pi} \phi^*(t) \sin nt dt. \end{aligned}$$

Remembering that

$$\phi^*(t) = \phi\left(\frac{Lt}{2\pi}\right) + t$$

and changing variables

$$\lambda = \frac{Lt}{2\pi},$$

we obtain

$$\begin{aligned} \mu_0 &= \frac{1}{L} \int_0^L \phi(\lambda) d\lambda + \pi, \\ a_n &= \frac{2}{L} \int_0^L \left(\phi(\lambda) + \frac{2\pi\lambda}{L}\right) \cos \frac{2\pi n\lambda}{L} d\lambda, \\ b_n &= \frac{2}{L} \int_0^L \left(\phi(\lambda) + \frac{2\pi\lambda}{L}\right) \sin \frac{2\pi n\lambda}{L} d\lambda. \end{aligned} \tag{5.1}$$

Exploiting the fact that $\phi(l)$ is a step function, the formulas for the Fourier coefficients are

$$\begin{aligned} \mu_0 &= -\pi - \frac{1}{L}\sum_{k=1}^{m} l_k \Delta\phi_k, \\ a_n &= -\frac{1}{n\pi}\sum_{k=1}^{m} \Delta\phi_k \sin\frac{2\pi n l_k}{L}, \\ b_n &= \frac{1}{n\pi}\sum_{k=1}^{m} \Delta\phi_k \cos\frac{2\pi n l_k}{L}, \end{aligned} \tag{5.2}$$

$$\text{where} \qquad l_k = \sum_{i=1}^{k} \Delta l_i.$$

The proof is given in the Appendix B1.

5.2 Modifications and Improvements

Fourier descriptors introduced by Zahn and Roskies are derived from the signature $\phi(l)$ linearized in the interval $[0, 2\pi]$ to $\phi^*(t)$, where linearization means adding the term t to $\phi(Lt/2\pi)$. Note that linearization ensures the continuity of $\phi^*(t)$ at $t = 0$ and $t = 2\pi$ but does not remove discontinuity of $\phi(l)$ inside the interval $[0, L]$. Instead of linearizing, which does not improve things much, Fourier descriptors can be derived from the step signature $\hat{\phi}(l)$, STZR, normalized in the interval $[0, 2\pi]$. The STZR descriptors are invariant to affine transformations.

5.2.1 Step Signature

Let γ be a polygonal curve with m vertices $V_0, V_1, \ldots, V_{m-1}, V_m = V_0$ and edges (V_{i-1}, V_i) of length $\Delta l_i, i = 1, \ldots, m (\Delta l_0 = 0)$. Let the angular change of direction at vertex V_i be $\Delta\phi_i$ (negative in clockwise direction and positive in counter clockwise direction) as shown in Figure 5.1b and $L = \sum_{i=1}^{m} \Delta l_i$. Define $l_i = \sum_{j=1}^{i} \Delta l_j, l_0 = 0$. Since the tangent line is undefined at the vertices of the polygon, the value

$$\frac{\lim_{s\uparrow l} \hat{\phi}(s) + \lim_{s\downarrow l} \hat{\phi}(s)}{2}$$

is assigned to $\hat{\phi}$ at the values of l corresponding to the vertices and this is the value

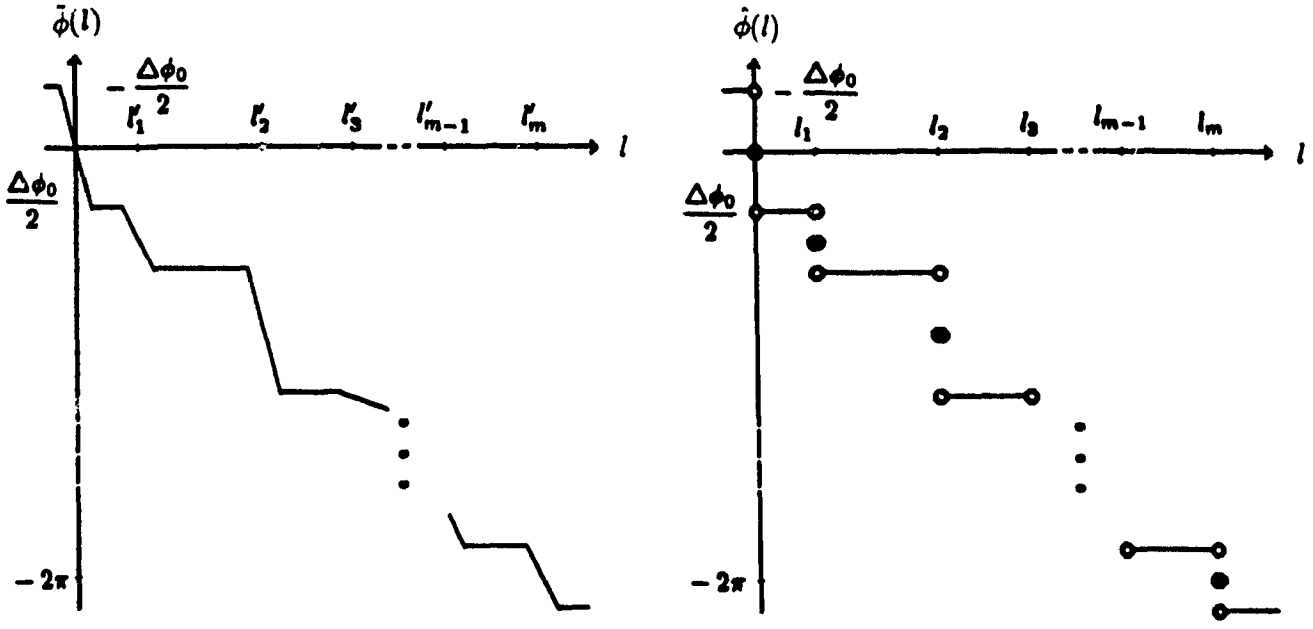

(a) Smoothed signature $\tilde{\phi}(l)$. (b) The Step signature $\hat{\phi}(l)$.

Figure 5.2: Step and Smoothed signature.

to which the Fourier series of $\hat{\phi}$ converges at the vertices. It is also assumed that

$$\hat{\theta}(0) = \lim_{l \downarrow 0} \hat{\theta}(l) - \frac{\Delta\phi_0}{2} = \hat{\delta}_0$$

and

$$\hat{\phi}(l) = \begin{cases} -\frac{\Delta\phi_0}{2} & \text{for} \quad -\delta < l < 0, \\ -2\pi + \frac{\Delta\phi_0}{2} & \text{for} \quad l_m < l < l_m + \delta \end{cases}$$

as shown in Figure 5.2b. Exploiting the fact that $\hat{\phi}(l)$ is a step function

$$\hat{\phi}(t) = \hat{\mu}_0 + \sum_{n=1}^{\infty} (\hat{a}_n \cos nt + \hat{b}_n \sin nt)$$

where $t = 2\pi l/L$. STZR descriptors are obtained after tedious but straightforward calculations as follows

$$\hat{A}_n = (\hat{a}_n^2 + \hat{b}_n^2)^{\frac{1}{2}}, \qquad \hat{\alpha}_n = \arctan \frac{\hat{b}_n}{\hat{a}_n}, \quad \hat{a}_n \neq 0,$$

where

$$\begin{aligned}
\hat{\mu}_0 &= -2\pi - \frac{1}{L}\sum_{k=1}^{m} l_k \Delta\phi_k + \frac{\Delta\phi_0}{2} = \mu_0 - \pi + \frac{\Delta\phi_0}{2}, \\
\hat{a}_n &= -\frac{1}{n\pi}\sum_{k=1}^{m} \Delta\phi_k \sin\frac{2\pi n l_k}{L} = a_n, \\
\hat{b}_n &= \frac{1}{n\pi}\sum_{k=1}^{m} \Delta\phi_k \cos\frac{2\pi n l_k}{L} + \frac{2}{n} = b_n + \frac{2}{n},
\end{aligned} \tag{5.3}$$

where μ_0, a_n and b_n are Fourier coefficients of ϕ^* from previous section. The proof of equation (5.3) is similiar to the proof of equation (5.2) and is omitted.

One of the most important justifications for the use of Fourier descriptors is the invariance of harmonic amplitudes, $\hat{A}_n$, under affine transformations and shifts of the starting point. The algebraic properties of STZR descriptors are summarized in the following theorem. It is clear that closed curves which differ only in position, orientation and size, but have analogous starting points are mapped into the same angular bend function and therefore have identical Fourier descriptors. For that reason, only shifts in the starting point and mirror reflections are considered.

Theorem 5.1 *If γ and γ' are two curves which only differ by Δl in the starting points Z_0 and Z_0', the Fourier descriptors $(\hat{A}_n, \hat{\alpha}_n)$ and $(\hat{A}'_n, \hat{\alpha}'_n)$ for γ and γ' satisfy*

$$\begin{aligned}
1.\ \hat{A}'_n &= \hat{A}_n, \\
2.\ \hat{\alpha}'_n &= \hat{\alpha}_n - n\Delta t, \\
3.\ \hat{\mu}'_0 &= \hat{\mu}_0 + \hat{\delta}_0 - \hat{\delta}'_0,
\end{aligned}$$

where

$$\Delta t = \frac{2\pi}{L}\Delta l.$$

If γ and γ' have identical starting points but are mirror reflections of one another then

$$\begin{aligned}
1.\ \hat{A}'_n &= \hat{A}_n, \\
2.\ \hat{\alpha}'_n &= -\hat{\alpha}_n, \\
3.\ \hat{\mu}'_0 &= -2\pi - \hat{\mu}_0.
\end{aligned}$$

Proof If γ and γ' differ by Δl in the starting point (in units of arc length clockwise from Z to Z') then $\hat{\theta}'(l) = \hat{\theta}(l + \Delta l)$. This implies that $\hat{\phi}'(l) + \hat{\delta}'_0 = \hat{\phi}(l + \Delta l) + \hat{\delta}_0$. Define $\hat{\phi}_*$, the normalized version of $\hat{\phi}$ to the interval $[0, 2\pi]$, as $\hat{\phi}_*(t) = \hat{\phi}(Lt/2\pi)$, we have

$$\hat{\phi}'_*(t) + \hat{\delta}'_0 = \hat{\phi}_*(t + \Delta t) + \hat{\delta}_0. \tag{5.4}$$

Expanding both $\hat{\phi}'_*$ and $\hat{\phi}_*(t + \Delta t)$ as a Fourier series

$$\begin{aligned} \hat{\phi}'_*(t) &= \hat{\mu}'_0 + \sum_{n=1}^{\infty} \hat{A}'_n \cos(nt - \hat{\alpha}'_n), \\ \hat{\phi}_*(t + \Delta t) &= \hat{\mu}_0 + \sum_{n=1}^{\infty} \hat{A}_n \cos(nt - (\hat{\alpha}_n - n\Delta t)). \end{aligned}$$

Equation (5.4) and the above equations imply the first part of the theorem.

In order to show the second part, notice that the curvature of γ at $Z(l)$ is equal to the curvature of γ' at $Z'(L - l)$ because reflection of the curve changes the sign of curvature but the change of orientation also changes the sign resulting in no net change. Therefore the cumulative angular change between 0 and l on γ is the same as between L and $L - l$ on γ'. So

$$\hat{\phi}'(L - l) + \hat{\phi}(l) = -2\pi.$$

This in turn implies that

$$\hat{\phi}'_*(2\pi - t) + \hat{\phi}_*(t) = -2\pi. \tag{5.5}$$

Since $\hat{\phi}'_*$ is periodic, $\hat{\phi}'_*(2\pi - t) = \hat{\phi}'_*(-t)$ and equation (5.5) may be written as

$$\hat{\phi}'_*(-t) + \hat{\phi}_*(t) = -2\pi. \tag{5.6}$$

Expanding $\hat{\phi}'_*(-t)$ and $\hat{\phi}_*(t)$ as a Fourier series

$$\begin{aligned} \hat{\phi}'_*(-t) &= \hat{\mu}'_0 + \sum_{n=1}^{\infty} \hat{A}'_n \cos(-nt - \hat{\alpha}'_n), \\ \hat{\phi}_*(t) &= \hat{\mu}_0 + \sum_{n=1}^{\infty} \hat{A}_n \cos(nt - \hat{\alpha}_n), \end{aligned}$$

equation (5.6) and the above equations imply the second part of the theorem.

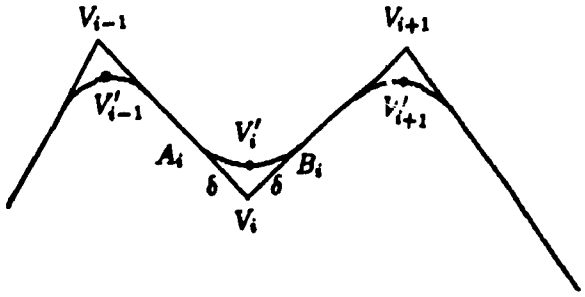

Figure 5.3: A polygonal curve and its smoothed quasipolygonal version.

5.2.2 Smoothed Signature

Both the ZR and STZR descriptors discussed so far are derived from discontinuous signature, resulting in the lack of uniform convergence of the Fourier series. To remedy this situation, a smoothed signature, SZR, is considered as follows

Definition 5.1 *Consider a closed polygonal curve γ with vertices $V_0, \ldots, V_{m-1}$, $V_m = V_0$ as shown in Figure 5.3. Smoothing of γ of order δ is obtained by inserting circular arcs $T_i = A_i V'_i B_i$, $i = 0, \ldots, m-1$ of length $\Delta l'_i = \delta |\Delta\phi_i| \cot(|\Delta\phi_i|/2)$ into angular corners so that the resulting quasipolygonal curve γ' is differentiable everywhere.*

The arc centers V'_i are arbitrary assumed corresponding to the polygonal vertices $V_i, i = 0, 1, \ldots, m-1$. The equation of the circle containing the circular arc T_i is determined as follows. The circle has radius $r_i = \delta \cot(|\Delta\phi_i|/2)$, with center (g_i, f_i). Notice that lines (V_{i-1}, V_i) and (V_i, V_{i+1}) are tangent to the circular arc T_i at points $P = (x_p, y_p)$ and $Q = (x_q, y_q)$ respectively, where

$$x_p = \frac{(\Delta l_i - \delta)x_i + \delta x_{i-1}}{\Delta l_i},$$
$$y_p = \frac{(\Delta l_i - \delta)y_i + \delta y_{i-1}}{\Delta l_i}$$

and

$$x_q = \frac{(\Delta l_{i+1} - \delta)x_i + \delta x_{i+1}}{\Delta l_{i+1}},$$
$$y_q = \frac{(\Delta l_{i+1} - \delta)y_i + \delta y_{i+1}}{\Delta l_{i+1}}$$

and

$$V_i = (x_i, y_i), \qquad \delta \leq \frac{(\min \Delta l_i)}{2}, \qquad \text{for} \quad 0 \leq i \leq m-1.$$

The equations of the tangents from the point V_i touching the circle at P and Q are

$$x_i x_p + y_i y_p - x_i g_i - x_p g_i - y_i f_i - y_p f_i + c_i = 0$$

and

$$x_i x_q + y_i y_q - x_i g_i - x_q g_i - y_i f_i - y_q f_i + c_i = 0$$

where

$$c_i = g_i^2 + f_i^2 - r_i^2.$$

Substracting the above equations, we get

$$(x_p - x_q)g_i + (y_p - y_q)f_i = -x_i(x_q - x_p) - y_i(y_q - y_p).$$

The slope of the tangent at Q is $-(x_q - g_i)/(y_q - f_i)$, therefore

$$(x_i - x_q)g_i + (y_i - y_q)f_i = -y_q(y_q - y_i) - x_q(x_q - x_i).$$

Solving the last two equations for f_i and g_i, the equation of the required circle which contains the circular arc T_i is

$$x^2 + y^2 - 2g_i x - 2f_i y + c_i = 0.$$

The lengths of the inserted circular arcs $T_i, i = 0, \ldots, m-1$ are smaller then the lengths of the corresponding angular corners $A_i V_i B_i$. Consequently, a closed contour γ' of length $L' = L - 2m\delta + \sum_{i=1}^{m} \Delta l_i'$, which is less than the length L of γ, is obtained. The signature $\tilde{\phi}(l)$ of the smoothed polygon can be obtained by smoothing the cumulative angular bend $\phi(l)$. The signature $\tilde{\phi}$ in Figure 5.2a is obtained by applying a smoothing operator $S[f]$ of order δ, as defined below, to ϕ in Figure 5.2b.

Operator S cannot be defined by a single equation since smoothing at the jump discontinuity requires scaling due to the change of length of the resulting curve. Scaling is not required outside the interval. Let $\delta \leq (\min \Delta l_i)/2$ for $1 \leq i \leq m$, then

$$\text{for} \quad x \in [l_{i-1} + \delta, l_i - \delta], \qquad i = 1, \ldots, m,$$
$$S[\hat{\phi}(x)] = \tilde{\phi}(x'), \tag{5.7}$$

where

$$x' = l'_{i-1} + \delta'_{i-1} + x - l_{i-1} - \delta, \qquad \delta'_i = \frac{\Delta l'_i}{2},$$

$$\text{for} \quad x \in [0, \delta] \cup [l_i - \delta, l_i + \delta] \cup [l_m - \delta, l_m], i = 1, \ldots, m-1,$$
$$S[\hat{\phi}(x)] = \tilde{\phi}(x') = \frac{1}{2\delta} \int_{x-\delta}^{x+\delta} \phi(l) dl, \tag{5.8}$$

where

$$x' = c_i[x - (l_i - \delta)] + (l'_i - \delta'_i), \qquad c_i = \frac{\delta'_i}{\delta}.$$

The degree of smoothing is controlled by δ, the large the δ is, the greater is the degree of smoothing [10].

Lemma 5.1

$$S[\hat{\phi}] = \tilde{\phi}.$$

Proof The case $x \in [l_{i-1} + \delta, l_i - \delta]$ is trivial and will be omitted. The case $x \in [0, \delta] \cup [l_i - \delta, l_i + \delta] \cup [l_m - \delta, l_m], i = 1, \ldots, m-1$ is proved.

When $x \in [0, \delta]$,

$$\begin{aligned} \tilde{\phi}(x') &= \frac{1}{2\delta} \left[\int_{x-\delta}^{0} -\frac{\Delta\phi_0}{2} dl + \int_0^{x+\delta} \frac{\Delta\phi_0}{2} dl \right] \\ &= \Delta\phi_0 (\frac{x}{2\delta}) \\ &= \frac{\Delta\phi_0}{\Delta l'_m} x'. \end{aligned}$$

When $x \in [l_i - \delta, l_i + \delta]$,

$$\begin{aligned} \tilde{\phi}(x') &= \frac{1}{2\delta} \left[\int_{x-\delta}^{l_i} \sum_{j=1}^{i-1} (\Delta\phi_j + \frac{\Delta\phi_0}{2}) dl + \int_{l_i}^{x+\delta} \sum_{j=1}^{i} (\Delta\phi_j + \frac{\Delta\phi_0}{2}) dl \right] \\ &= \frac{\Delta\phi_0}{2} + \sum_{j=1}^{i-1} \Delta\phi_j + \frac{\Delta\phi_i}{2\delta'} (x' - (l'_i - \delta'_i)) \\ &= \frac{\Delta\phi_i}{\Delta l'_i} x' + \frac{\Delta\phi_0}{2} + \sum_{j=1}^{i} \Delta\phi_j + \frac{\Delta\phi_i}{2} - \frac{\Delta\phi_i}{\Delta l'_i} l'_i. \end{aligned}$$

When $x \in [l_m - \delta, l_m]$,

$$\begin{aligned}\tilde{\phi}(x') &= \frac{1}{2\delta}\left[\int_{x-\delta}^{l_m}(-2\pi - \frac{\Delta\phi_m}{2})dl + \int_{l_m}^{x+\delta}(-2\pi + \frac{\Delta\phi_m}{2})dl\right] \\ &= -2\pi - \frac{\Delta\phi_m}{2\delta}(l_m + x) \\ &= \frac{\Delta\phi_m}{\Delta l'_m}x' - (2\pi + \frac{\Delta\phi_m}{\Delta l'_m}l'_m).\end{aligned}$$

This ends the proof.

SZR is a continuous function in the interval $0 \leq l \leq L'$, where L' is the length of the quasipolygonal curve. The Fourier descriptors $\{\tilde{A}_n, \tilde{\alpha}_n\}$ are calculated for the polygonal contours by expanding $\tilde{\phi}(l)$ as a Fourier series in the amplitude-phase form

$$\tilde{\phi}(l) = \tilde{\mu}_0 + \sum_{n=1}^{\infty} \tilde{A}_n \cos(nt - \tilde{\alpha}_n)$$

which is equivalent to

$$\tilde{\phi}(l) = \tilde{\mu}_0 + \sum_{n=1}^{\infty} (\tilde{a}_n \cos nt + \tilde{b}_n \sin nt)$$

where

$$\tilde{A}_n = (\tilde{a}_n^2 + \tilde{b}_n^2)^{\frac{1}{2}}, \qquad \tilde{\alpha}_n = \arctan\frac{\tilde{b}_n}{\tilde{a}_n}, \quad n = 1, 2, \ldots,$$

provided that $\tilde{a}_n \neq 0$.

The coefficient $\tilde{\mu}_0, \tilde{a}_n$ and $\tilde{b}_n$ are given by

$$\begin{aligned}\tilde{\mu}_0 &= -\frac{1}{L'}\sum_{i=1}^{m} l'_i \Delta\phi_i - 2\pi + \frac{\Delta\phi_m}{2}, \\ \tilde{a}_n &= -\frac{1}{n\pi}\left[\frac{L'}{n\pi}\sum_{i=1}^{m}\frac{\Delta\phi_i}{\Delta l'_i}\sin\frac{2\pi n l'_i}{L'}\sin\frac{\pi n \Delta l'_i}{L'}\right], \\ \tilde{b}_n &= \frac{1}{n\pi}\left[\frac{L'}{n\pi}\sum_{i=1}^{m}\frac{\Delta\phi_i}{\Delta l'_i}\cos\frac{2\pi n l'_i}{L'}\sin\frac{\pi n \Delta l'_i}{L'} + 2\pi\right].\end{aligned} \tag{5.9}$$

The proof is given in the Appendix B2. SZR descriptors behave similiarily to STZR descriptors under affine transformations. The results are summarized in next theorem. The proof is similar to the proof of theorem 5.1 and is omitted.

Theorem 5.2 *If γ and γ' are two curves which differ by Δl in the starting points Z_0 and Z_0' then $(\tilde{A}_n, \tilde{\alpha}_n)$ and $(\tilde{A}_n', \tilde{\alpha}_n')$ for γ and γ' satisfy*

$$\begin{aligned} 1.\ \tilde{A}_n' &= \tilde{A}_n, \\ 2.\ \tilde{\alpha}_n' &= \tilde{\alpha}_n - n\Delta t, \\ 3.\ \tilde{\mu}_0' &= \tilde{\mu}_0 + \tilde{\delta}_0 - \tilde{\delta}_0', \end{aligned}$$

where

$$\Delta t = \frac{2\pi\Delta l}{L'}.$$

If γ and γ' are mirror reflection of one another then

$$\begin{aligned} 1.\ \tilde{A}_n' &= \tilde{A}_n, \\ 2.\ \tilde{\alpha}_n' &= -\tilde{\alpha}_n, \\ 3.\ \tilde{\mu}_0' &= -\tilde{\mu}_0 - 2\pi. \end{aligned}$$

SZR has one disadvantage, its periodic extension into the whole real line still has jump discontinuities at multiplicities of L' because $\tilde{\phi}(0) = 0 \neq \tilde{\phi}(L') = -2\pi$. To remove these discontinuities, a linearized, smoothed signature, LSZR, normalized in the interval $[0, 2\pi]$ is introduced.

5.2.3 Linearized Smoothed Signature

The linearized smoothed signature, LSZR, is defined as follow

$$\tilde{\phi}^*(t) = \tilde{\phi}\left(\frac{L't}{2\pi}\right) + t.$$

Signature $\tilde{\phi}^*(t)$ is invariant under translations, rotations and scaling. Expand $\tilde{\phi}^*$ as a Fourier series

$$\tilde{\phi}^*(t) = \tilde{\mu}_0^* + \sum_{n=1}^{\infty}(\tilde{a}_n^* \cos nt + \tilde{b}_n^* \sin nt).$$

In polar form, the expansion is

$$\tilde{\phi}^*(t) = \tilde{\mu}_0^* + \sum_{n=1}^{\infty} \tilde{A}_n^* \cos(nt - \tilde{\alpha}_n^*)$$

where the Fourier coefficients of the signature are calculated by the following formulas

$$\begin{aligned}\tilde{\mu}_0^* &= \frac{1}{2\pi}\int_0^{2\pi}\tilde{\phi}^*(t)dt,\\ \tilde{a}_n^* &= \frac{1}{\pi}\int_0^{2\pi}\tilde{\phi}^*(t)\cos ntdt,\\ \tilde{b}_n^* &= \frac{1}{\pi}\int_0^{2\pi}\tilde{\phi}^*(t)\sin ntdt.\end{aligned}$$

After straightfroward calculations, we obtain the following relationships between the Fourier coefficients of $\tilde{\phi}$ and $\tilde{\phi}^*$

$$\tilde{\mu}_0^* = \tilde{\mu}_0 + \pi, \qquad \tilde{a}_n^* = \tilde{a}_n, \qquad \tilde{b}_n^* = \tilde{b}_n - \frac{2}{n}.$$

Obviously, $\tilde{a}_n^*$ and $\tilde{b}_n^*$ are functions of δ and they converge to ZR Fourier coefficients as $\delta \to 0$. Fourier descriptors corresponding to LSZR are defined as follows

$$\tilde{A}_n^* = (\tilde{a}_n^{*2} + \tilde{b}_n^{*2})^{\frac{1}{2}}, \qquad \tilde{\alpha}_n^* = \arctan\frac{\tilde{b}_n^*}{\tilde{a}_n^*}, \qquad n = 1, 2, \ldots,$$

provided that $\tilde{a}_n^* \neq 0$.

LSZR descriptors behave similiary to STZR descriptors under affine transformation. The result are summarized in the next theorem, where the proof is similiar to the proof of theorem 5.1 and is omitted.

Theorem 5.3 *If γ and γ' are two curves which differ by Δl in the starting point Z_0 and Z_0' then $(\tilde{A}_n^*, \tilde{\alpha}_n^*)$ and $(\tilde{A}_n^{*'}, \tilde{\alpha}_n^{*'})$ for γ and γ' satisfy*

$$\begin{aligned}1.\ \tilde{A}_n^{*'} &= \tilde{A}_n^*,\\ 2.\ \tilde{\alpha}_n^{*'} &= \tilde{\alpha}_n^* - n\Delta t,\\ 3.\ \tilde{\mu}_0^{*'} &= \tilde{\mu}_0^* + \tilde{\delta}_0^* - \tilde{\delta}_0^{*'} - \Delta t,\end{aligned}$$

where

$$\Delta t = \frac{2\pi\Delta l}{L'}.$$

If γ and γ' are mirror reflection of one another then

$$\begin{aligned}1.\ \tilde{A}_n^{*'} &= \tilde{A}_n^*,\\ 2.\ \tilde{\alpha}_n^{*'} &= -\tilde{\alpha}_n^*,\\ 3.\ \tilde{\mu}_0^{*'} &= -\tilde{\mu}_0^*.\end{aligned}$$

In order to see how much information that the Fourier descriptors contain, different number of Fourier descriptors are used to reconstructed the closed polygonal curve and the results are presented in next chapter.

Chapter 6

Examples and Reconstructions

An example illustrating derivation of formulas for different types of Fourier coefficients is given. The reconstruction formulas for the polygonal curve are derived. Experiments are performed to test how much information is contained in the first few Fourier descriptors contain and the results are presented.

6.1 Example

Formulas for different Fourier coefficients are derived for an equilateral triangular contour as shown in Figure 6.1a and Figure 6.1b. Figure 6.1b is the smoothed equilateral triangular contour of Figure 6.1a. Figure 6.2a and Figure 6.2b show the cumulative angular bend functions $\hat{\phi}$ and $\tilde{\phi}$ for the contours from Figure 6.1a and Figure 6.1b respectively. The perimeters of the triangle and the smoothed triangle are $3a$ and $3a'$ respectively, where

$$3a' = 3a - 6\delta + \frac{2\pi}{\sqrt{3}}\delta.$$

According to equation (5.3), the STZR Fourier coefficients are given by the formulas

$$\begin{aligned}
\hat{\mu}_0 &= -\pi, \\
\hat{a}_n &= 0, \\
\hat{b}_n &= \begin{cases} \frac{2}{3n}(2+\cos\frac{n\pi}{3}) & \text{when } n \text{ is odd} \\ \frac{2}{3n}(2-\cos\frac{n\pi}{3}) & \text{when } n \text{ is even} \end{cases} \qquad \text{for } n = 1, 2, \ldots.
\end{aligned}$$

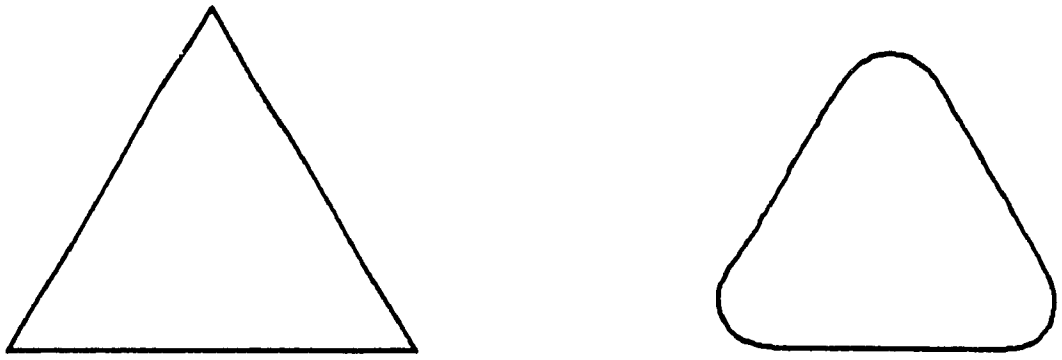

(a) Equilaterial triangle. (b) Smoothed equilaterial triangle.

Figure 6.1: Equilaterial and smoothed equilaterial triangles.

From equation (5.2), the ZR Fourier coefficients are given by the formulas

$$\begin{aligned} \mu_0 &= \frac{\pi}{3}, \\ a_n &= 0, \\ b_n &= \begin{cases} -\frac{2}{3n}(1-\cos\frac{n\pi}{3}) & \text{when } n \text{ is odd} \\ -\frac{2}{3n}(1+\cos\frac{n\pi}{3}) & \text{when } n \text{ is even} \end{cases} \quad \text{for } n = 1,2,\ldots. \end{aligned}$$

By equation (5.9), the SZR Fourier coefficients are given by the formulas

$$\begin{aligned} \tilde{\mu}_0 &= -\pi, \\ \tilde{a}_n &= 0, \\ \tilde{b}_n &= \begin{cases} \frac{2}{n}(1-\frac{1}{n\pi}(1-\cos\frac{n\pi}{3})\sin\frac{n\pi}{3}) & \text{when } n \text{ is odd} \\ \frac{2}{3n}(1-\frac{1}{n\pi}(1+\cos\frac{n\pi}{3})\sin\frac{n\pi}{3}) & \text{when } n \text{ is even} \end{cases} \quad \text{for } n = 1,2,\ldots. \end{aligned}$$

From the relationship between SZR and LSZR descriptors, the formulas for LSZR Fourier coefficients are

$$\begin{aligned} \tilde{\mu}_0^* &= 0, \\ \tilde{a}_n^* &= 0, \\ \tilde{b}_n^* &= \begin{cases} -\frac{2}{n^2\pi}(1-\cos\frac{n\pi}{3})\sin\frac{n\pi}{3} & \text{when } n \text{ is odd} \\ -\frac{2}{n^2\pi}(1+\cos\frac{n\pi}{3})\sin\frac{n\pi}{3} & \text{when } n \text{ is even} \end{cases} \quad \text{for } n = 1,2,\ldots. \end{aligned}$$

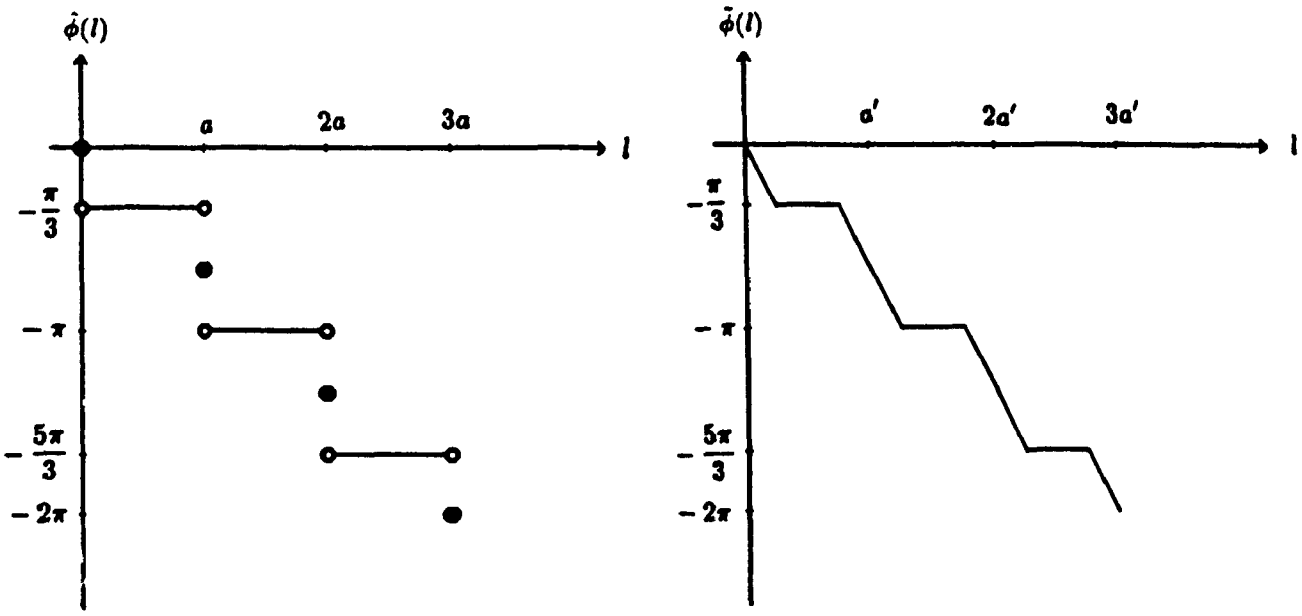

(a) Step signature of the triangle. (b) Smoothed signature of the triangle.

Figure 6.2: Step and smoothed signature of equilaterial triangles.

6.2 Reconstruction

Having developed the descriptors, it is of interest to know how easily the curve might be reconstructed from these descriptors. The following theorem gives the reconstruction formula.

Theorem 6.1 *If γ is described by $\theta(l)$ and the starting point $Z(0)$, the position of the point $Z(l)$ can be obtained from the expression*

$$Z(l) = Z(0) + \int_0^l \exp(i\theta(\lambda))d\lambda \tag{6.1}$$

which is equivalent to

$$x(l) = x(0) + \int_0^l \cos\theta(\lambda)d\lambda,$$
$$y(l) = y(0) + \int_0^l \sin\theta(\lambda)d\lambda.$$

Proof By definition $\theta(l)$ measures the direction of the velocity vector $\gamma'(l) = (x'(l), y'(l))$ which is tangent to γ at l. Whenever a curve is parameterized by its arc

length the speed $|\gamma'(l)|$ is always 1 and $x'(l) = \cos\theta(l)$, $y'(l) = \sin\theta(l)$. The result follows by substituting these values into the fundamental theorem of integral calculus

$$x(l) - x(0) = \int_0^l x'(\lambda)d\lambda,$$
$$y(l) - y(0) = \int_0^l y'(\lambda)d\lambda.$$

Using Theorem 6.1, we obtain the following reconstruction formula for the linearized signature approximated by the first N terms of the Fourier expansion

$$Z(l) = Z(0) + \frac{L}{2\pi}\int_0^{\frac{2\pi l}{L}} \exp\left\{i\left[-t + \delta_0 + \mu_0 + \sum_{k=1}^{N}(a_k \cos kt + b_k \sin kt)\right]\right\} dt.$$

Similiarily, the reconstruction formula for non linearized signature is

$$Z(l) = Z(0) + \frac{L}{2\pi}\int_0^{\frac{2\pi l}{L}} \exp\left\{i\left[\delta_0 + \mu_0 + \sum_{k=1}^{N}(a_k \cos kt + b_k \sin kt)\right]\right\} dt.$$

A number of experiments on a set of digitized handwritten characters selected from Suen's database [27] was performed using ZR and LSZR descriptors. The number of points for reconstruction was 100. The experiments were performed on Sun 3/50 workstation. The characters '1', '3', '5' and '9' were used. Different number of Fourier descriptors were used for reconstruction. Figure 6.3 through Figure 6.6 show reconstructed characters using 5, 13, 25 and 65 ZR descriptors respectively and Figure 6.7 through Figure 6.10 show reconstructed characters using 5, 13, 25 and 65 LSZR descriptors. It can be seen that LSZR descriptors contain more informations about contours than ZR descriptors. This is due to the fact that LSZR descriptors are derived from continuous signatures. Therefore, the LSZR descriptors are well suited for the reconstruction and the encoding of shape features and for applications in shape classification. For more details on LSZR and other descriptors refer to [24] [25] [26].

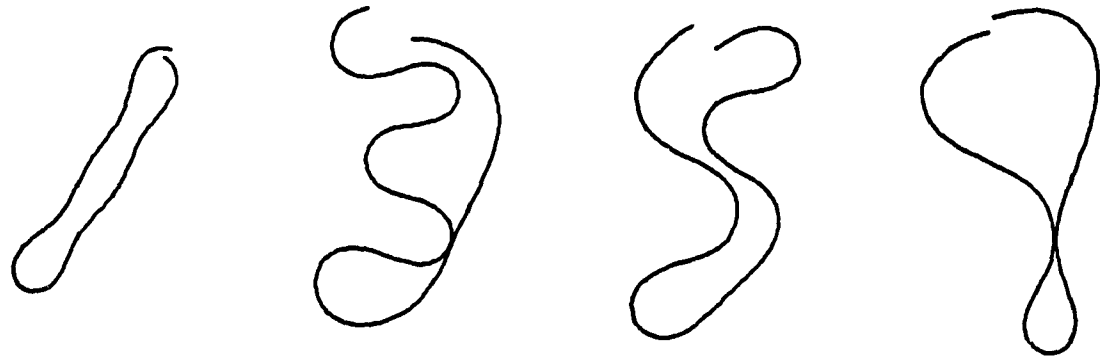

Figure 6.3: Reconstructed Shapes:Using 5 ZR descriptors.
Characters '1', '3', '5', and '9'.

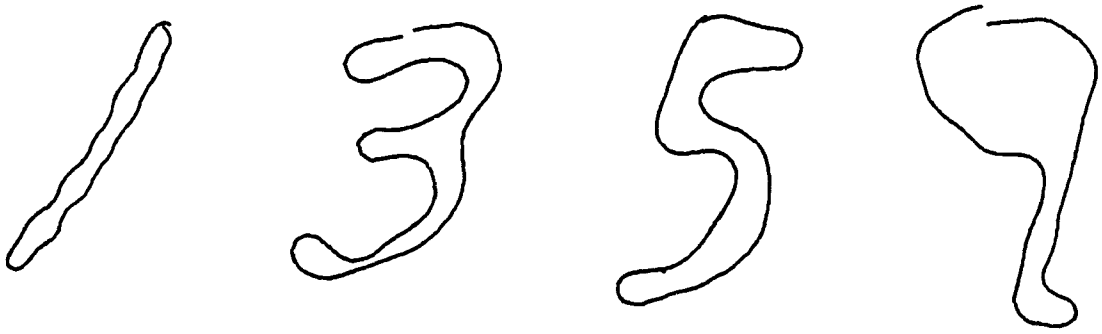

Figure 6.4: Reconstructed Shapes:Using 13 ZR descriptors.
Characters '1', '3', '5', and '9'.

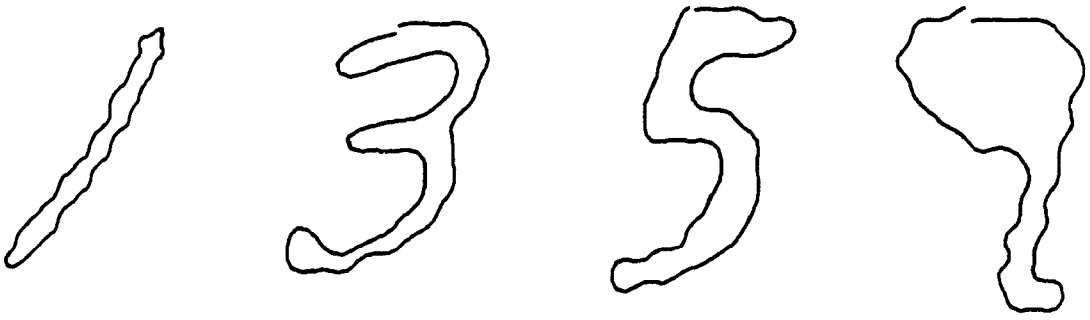

Figure 6.5: Reconstructed Shapes:Using 25 ZR descriptors.
Characters '1', '3', '5', and '9'.

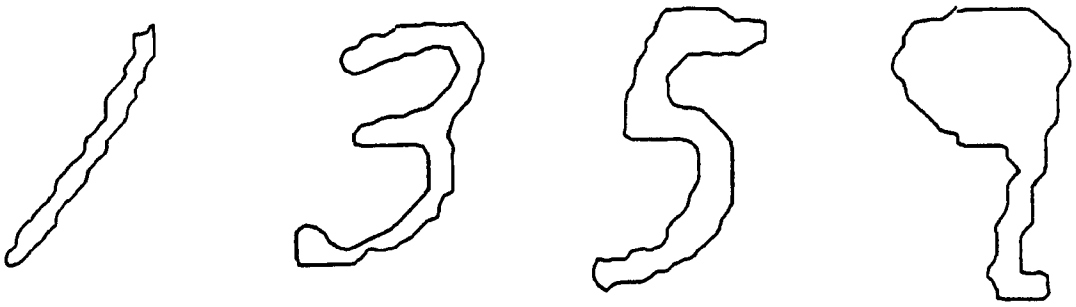

Figure 6.6: Reconstructed Shapes:Using 65 ZR descriptors.
Characters '1', '3', '5', and '9'.

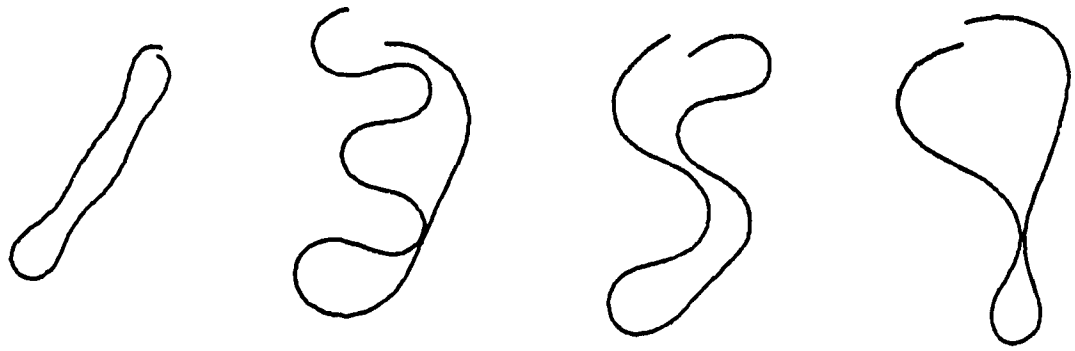

Figure 6.7: Reconstructed Shapes:Using 5 LSZR descriptors.
Characters '1', '3', '5', and '9'.

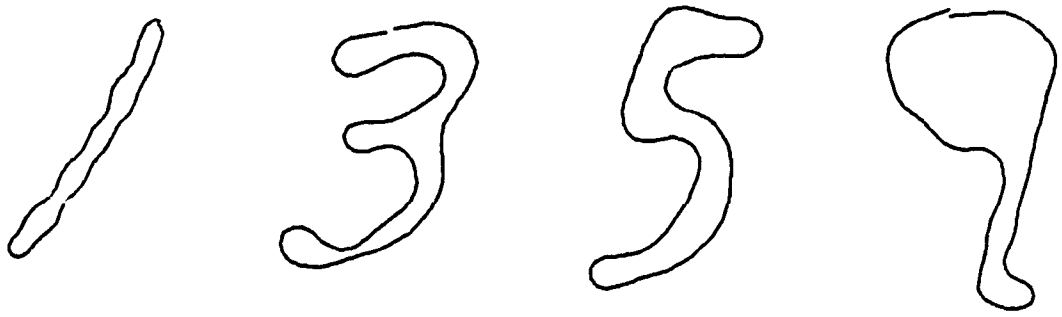

Figure 6.8: Reconstructed Shapes:Using 13 LSZR descriptors.
Characters '1', '3', '5', and '9'.

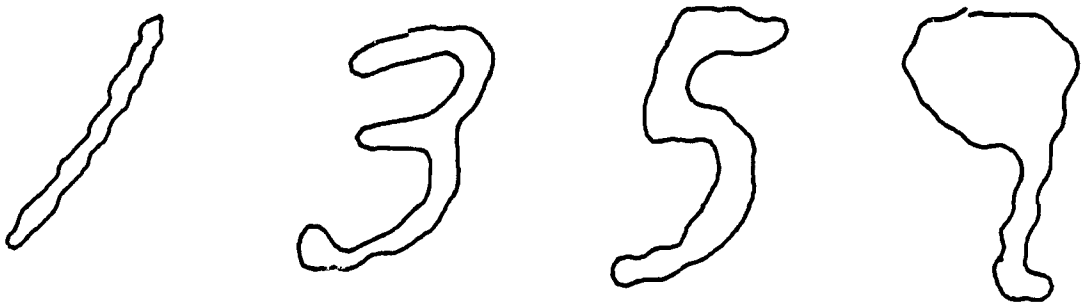

Figure 6.9: Reconstructed Shapes:Using 25 LSZR descriptors.
Characters '1', '3', '5', and '9'.

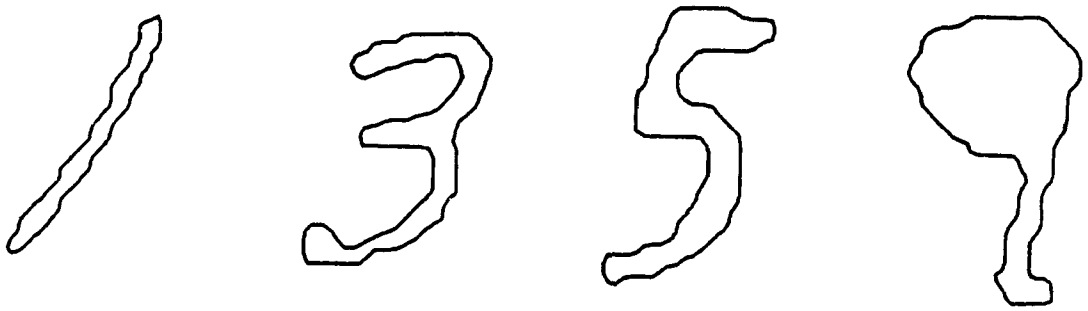

Figure 6.10: Reconstructed Shapes:Using 65 LSZR descriptors.
Characters '1', '3', '5', and '9'.

Conclusion

In this thesis, we studied coding and reconstruction of two dimensional closed contours using statistical and deterministic descriptors. First, we applied circular ARMA model to encode discrete boundary points. We estimated parameters of the model and chose its optimal order. This approach generalizes the approaches based on the circular AR models. We found out that the parameters and their estimates of the model are invariant to scaling and shifts of the starting point. The results of simulation show that the estimates of the parameters carry significant statistical information about the shapes. As the number of quantization levels decreases, the quality of the reconstructed characters remains good. Simulation also show that the reconstruction process is not vary sensitive to the model order as long as the order does not differ much from the optimal order. Next, we applied Fourier descriptors to contour coding. New descriptors were derived and their properties were investigated. We tested both types of descriptors, ZR and LSZR descriptors, on handwritten numerals collected from the dead letter envelopes by the United States Post Office. We proved that the amplitudes of the Fourier descriptors are invariant to rotations, translations, scaling, mirror reflection and the shifts of the starting point. From the results of simulation, it can be seen that the LSZR descriptors contain more information about the contour than ZR descriptors because LSZR descriptors are derived from the continuous signatures. In the future, the boundary descriptors developed in this thesis will be applied to the classification of planar shapes.

Bibliography

[1] Bovas Abraham and Johannes Ledolter. *Statistical mathod for forecasting.* John Wiley & Sons, 1983.

[2] Hirotugu Akaike. *A New Look at the Statistical Model Identification.* IEEE Transactions on Automatic Control, Vol. AC-19, No. 6, december 1974.

[3] J. K. Beddow. *Particle morphological analysis.* in Advanced Particulate Morphology, J. K. Beddow and T. P. Meloy, Eds. Boca Raton, FL. : C.R.C., 1980, pp. 1-84.

[4] G. E. P. Box and G. M. Jenkines. *Time Series Analysis : forcasting and control.* Revised edition, Holden Day, 1976.

[5] Peter J. Brockwell and Richard A. Paris. *Time Series : Theory and Methods.* Springer Series in Statistics, Springer-Verlag, 1987.

[6] C. Chatfield. *The Analysis of Time Series : An Introduction.* Third edition, Chapman and Hall, 1984.

[7] L. Davis. *Shape matching using relaxation techniques* . IEEE Trans. Pattern Anal. Machine Intel., Vol. PAMI-1, January 1979, pp. 60-72.

[8] F. M. Dekking and P. J. Van Otterloo. *Fourier coding and reconstuction of complicated contours.* IEEE Trans. on Systems, Man, and Cybernetics, Vol. SMC-16, No. 3, May/June 1986, pp. 395-404.

[9] S. R. Dubois and F. H. Glanz. *An autoregressive mode approach to 2-d shape classification.* IEEE Trans. Pattern Anal. Machine Intel., Vol. PAMI-8, January 1986, pp. 55-56.

[10] R. O. Duda and P. E. Hart. *Pattern Classification and Scene Analysis.* New York : Wiley, 1973.

[11] S. A. Dudani et al. *Aircraft identification by movement invariants.* IEEE Trans. Comput., Vol. C-26, January 1977, pp.39-46.

[12] F. Etesami and J. J. Uicker, Jr.. *Automatic dimensio nal inspection of machine part cross-section using Fourier analysis.* Comput. Vision, Graphics, Image Process., Vol. 29, 1985, pp. 216-247.

[13] G. E. Forsythe, M.A. Malcolm and C. B. Mpler. *Computer methods for numerical computations.* Englwood Cliffs: Prentice Hall, 1977.

[14] K. S. Fu. *Syntactic Pattern Recongnition.* Prentice Hall, Englewood Cliffs, New Jersey, 1982.

[15] C. R. Giardina and F. P. Kuhl. *Accuracy of curve approximation by harmonically related vectors with ellipticall loci.* Comp. Graph. Image Proc. Vol. 6, 1977, pp. 277-285.

[16] L.Gupta and M.D.Srinath. *Invariant planar shape recognition using Dynamic Alignment.* Pattern Recognition Vol 21. No.3 pp 235-239, 1988.

[17] Rafael C. Gonzalez and Paul Wintz. *Digital Image Processing.* Second edition, Addison Wesley, 1987.

[18] G. H. Granlund. *Fourier preprocessing for hand print character recongnition.* IEEE Trans. Comp., Vol. C-21, 1972, pp. 195-201.

[19] Robert V. Hogg and Allen T. Craig. *Introduction to Mathematical Statistics.* Third edition, Macmillan Publishing Co., Inc., 1965.

[20] R. Nigel Horspool. *C Programming in the Berkeley Unix Environment.* Prentice-Hall, 1986.

[21] R. L. Kashyap and R. Chellappa. *Stochastic models for closed boundary analysis : representation and reconstruction.* IEEE Trans. Inform. Theory, Vol. IT-27, September 1981, pp. 627-637.

[22] Maurice Kendall, Alan Stuart and J. Keith Ord. *The Advanced Theory of Statistics.* Vol. 3, Fourth edition, Charles Griffin & Company Limited, 1983.

[23] A. Knopp. *Theory and Applicationc of Infinite Series.* New York, Hafner, 1974.

[24] A. Krzyzak, S.Y. Leung and C.Y. Suen. *Reconstruction of two dimensional patterns by Fourier descriptors.* Machine Vision and Applications Journal, Vol. 2, No 3, 1989, pp. 123-140.

[25] A. Krzyzak, S.Y. Leung and C.Y. Suen. *Reconstruction of two dimensional patterns by Fourier decriptors.* Proceedings of the 9th International Conference on Pattern Recongnition, Rome, November 14-17, 1988.

[26] A. Krzyzak, S.Y. Leung and C.Y. Suen. *Fourier descriptors of two dimensional shapes-reconstruction and accuracy.* Proceedings of the IAPR Workshop on Computer Vision-Special Hardware and Industrial Application, Tokyo, October 12-14, 1988.

[27] M. T. Y. Lai and C. Y. Suen. *Automatic recongnition of charatcters by Fourier descriptors and boundary line encodings.* Pattern Recongnition Vol. 14, No's. 1-6, 1981, pp. 383-393.

[28] Leslie Lamport. *Latex.* Addison-Wesley Publish Company, 1986.

[29] C. C. Lin and R. Chellappa. *Classification of partial 2-d shapes using Fourier descriptors.* Proc. IEEE Conf. Computer Vision and Pattern Recongnition, Miami Beach, 1986, pp. 344-350.

[30] J.Mantas. *Methodologies in Pattern Recognition and Image Analysis – A Brief Survey.* Pattern Recognition Vol 20. No.1 pp. 1-6, 1987.

[31] J. Max. *Quantization for minimum distortion.* IRE Trans. In-form. Theory, pp. 7-12, Mar. 1960.

[32] A. Oosterlink et al.. *Evaluation of diffenert profile description and decomposition methods for banded chromosomes.* In Proc. 3rd Int. Joint Conf. Pattern Recongnition, November 1976, pp. 334-338.

[33] J. O'Rourke, *The signature of a plane curve*, SIAM J. Comput., Vol. 15, No. 1, February 1986, pp. 34-51.

[34] Alan Pankratz. *Forecasting with Univariate Box - Jenkins Models.* John Wiley & Sons, 1983.

[35] T. Pavlidis and F. Ali. *A hierarchical syntactic shape analyzer.* IEEE Trans. Pattern Anal. Machine Intel., Vol. PAMI-1, January 1979, pp. 2-9.

[36] T. Pavlidis. *Algorithms for shape analysis of contours and waveforms.* IEEE Trans. Pattern Anal. Mach. Intell., Vol. PAMI-2, 1980, pp. 301-312.

[37] E. Persoon and K. S. Fu. *Shape discrimination using Fourier descriptors.* IEEE Trans. Syst. Man, Cybern. Vol. SMC-7, March 1977, pp. 170-179.

[38] William H. Press, Brain P. Flannery, Saul A. Teukolsky and William T. Vetterting. *Numerical Recipes in C.* Cambridge University Press, 1988.

[39] M. B. Priestley. *Spectral Analysis and Time Series.* Academic Press, 1981.

[40] C. W. Richard and H. Hemami. *Identification of three-dimensional objects using Fourier descriptors of the boundary curve.* IEEE Trans. Syst. Man, Cybern. Vol. SMC-4, July 1974, pp. 371-378.

[41] J. Strackee and N. J. D. Nagelkerrke. *On closing the Fourier descriptor presentation.* IEEE Trans. on Pattern Analysis and Machine Intelligence, Vol. PAMI-5, No. 6, November 1983.

[42] G. P. Tolstov, *Fourier Series*, Dover, New York, 1976.

[43] T. P. Wallace and P. A. Wintz. *An efficient three - dimensional aircraft recognition algorithm using normalized Fourier descriptors.* Computer Graphics and Image Processing, 13, 1980, pp. 99-126.

[44] Mitchell Waite, Stephen Prata and Donald Martin. *C Primer Plus.* Revised edition, Howard W. Sams & Company, 1987.

[45] C. T. Zahn and R. S. Roskies. *Fourier descriptors for plane closed curves.* IEEE Trans. Comput., Vol. C-21, March 1972, pp. 269-281.

[46] A. Zygmund. *Trigonometric Series.* Dover, New York 1955.

Appendix A

Some Useful Methods

A.1 Newton Raphson Method

Suppose we want to find a solution of a system of nonlinear equations

$$f_i(x_1, \ldots, x_N) = 0, \qquad i = 1, \ldots, N.$$

Let $\mathbf{X}$ denotes the entire vector of values x_i then, in the neighbourhood of $\mathbf{X}$, each of the functions f_i can be expanded into Taylor series

$$f_i(\mathbf{X} + \delta\mathbf{X}) = f_i(\mathbf{X}) + \sum_{j=1}^{N} \frac{\partial f_i}{\partial x_j} \delta x_j + O(\delta\mathbf{X}^2).$$

By neglecting terms of order $\delta\mathbf{X}^2$ and higher, a set of linear equations for the corrections $\delta\mathbf{X}$ is obtained

$$\sum_{j=1}^{N} \alpha_{ij}\, \delta x_j = \beta_i \qquad (A.1)$$

where

$$\alpha_{ij} = \frac{\partial f_i}{\partial x_j}, \qquad \beta_i = -f_i.$$

After equation(A.1) is solved, corrections are added to the current estimate of the solution

$$x_i^{new} = x_i^{old} + \delta x_i, \qquad i = 1, \ldots, N$$

after equation(A.1) is solved.

Iterations are containued until convergence is reached. That is until absloute difference between x_i^{new} and x_i^{old} is less than ε or until a specificed number of iterations,

k, has been taken. The partial derivatives needed in equation(A.1) can be calculated numerically by

$$\alpha_{ij} = \frac{f_i(x_1, \ldots, x_j + \delta, \ldots, x_N) - f_i(x_1, \ldots, x_j, \ldots, x_N)}{\delta}.$$

A.2 Laguerre's Method

Laguerre's method [38] is used to determine the roots of a polynomial. The method requires complex arithmetics (even while the roots are real), but it is guaranteed to converge to a root from any starting point.

The relations between the polynomial, its roots and derivatives are

$$P_n(x) = (x - x_1)(x - x_2)\cdots(x - x_n),$$

$$\ln|P_n(x)| = \ln|x - x_1| + \ln|x - x_2| + \cdots + \ln|x - x_n|,$$

$$\frac{d}{dx}\ln|P_n(x)| = \frac{1}{x - x_1} + \frac{1}{x - x_2} + \cdots + \frac{1}{x - x_n} = \frac{P_n'}{P_n} \equiv G, \tag{A.2}$$

$$-\frac{d^2}{dx^2}\ln|P_n(x)| = \frac{1}{(x - x_1)^2} + \frac{1}{(x - x_2)^2} + \cdots + \frac{1}{(x - x_n)^2} = \left[\frac{P_n'}{P_n}\right]^2 - \frac{P_n''}{P_n} \equiv H. \tag{A.3}$$

The root x_1 is assumed to be located some distance a from the current guess, while all other roots are assumed to be located at a distance b, where

$$a = x - x_1, \qquad b = x - x_i, \quad i = 2, 3, \ldots, n.$$

Equations (A.2) and (A.3) can be expressed as

$$\frac{1}{a} + \frac{n-1}{b} = G, \tag{A.4}$$

$$\frac{1}{a^2} + \frac{n-1}{b^2} = H, \tag{A.5}$$

which yield the solution for a, where

$$a = \frac{n}{G \pm \sqrt{(n-1)(nH - G^2)}}. \tag{A.6}$$

The sign in equation(A.6) is taken to yield the largest magnitude for the denominator. Since the factor inside the square root can be negative, a can be complex. The method operates iteratively : for a trial value x, a is calculated by equation (A.6). Then $x - a$ becomes the next trial value. This process is continued until a is sufficiently small.

Appendix B

Proof of the Lemmas

B.1 ZR Descriptors

Lemma B.1 *Let γ be a polygonal curve. The Fourier coefficients of ϕ are*

$$\begin{aligned}
\mu_0 &= -\frac{1}{L}\sum_{k=1}^{m} l_k \Delta\phi_k - \pi, \\
a_n &= -\frac{1}{n\pi}\sum_{k=1}^{m} \Delta\phi_k \sin\frac{2n\pi l_k}{L}, \\
b_n &= \frac{1}{n\pi}\sum_{k=1}^{m} \Delta\phi_k \cos\frac{2n\pi l_k}{L}.
\end{aligned}$$

Proof From equation (5.1)

$$\begin{aligned}
\mu_0 &= \frac{1}{L}\int_0^L \phi(\lambda)d\lambda + \pi \\
&= \frac{1}{L}\sum_{k=1}^{m-1}\int_{l_k}^{l_{k+1}} \sum_{j=1}^{k} \Delta\phi_j d\lambda + \pi \\
&= \frac{1}{L}\sum_{k=1}^{m-1}\left[(l_{k+1}-l_k)\sum_{j=1}^{k}\Delta\phi_j\right] + \pi \\
&= \frac{1}{L}\left[-\sum_{k=1}^{m-1} l_k\Delta\phi_k + l_m\sum_{j=1}^{m-1}\Delta\phi_j\right] + \pi \\
&= \frac{1}{L}\left[-2\pi l_m - \sum_{k=1}^{m} l_k\Delta\phi_k\right] + \pi.
\end{aligned}$$

$$
\begin{aligned}
a_n &= \frac{2}{L}\int_0^L \left(\phi(\lambda)+\frac{2\pi\lambda}{L}\right)\cos\frac{2n\pi\lambda}{L}d\lambda,\\
\frac{2}{L}\int_0^L \phi(\lambda)\cos\frac{2n\pi\lambda}{L}d\lambda &= \frac{2}{L}\sum_{k=1}^{m-1}\int_{l_k}^{l_{k+1}}\sum_{j=1}^{k}\Delta\phi_j\cos\frac{2n\pi\lambda}{L}d\lambda\\
&= \frac{1}{n\pi}\sum_{k=1}^{m-1}\left[\sum_{j=1}^{k}\Delta\phi_j(\sin\frac{2n\pi l_{k+1}}{L}-\sin\frac{2n\pi l_k}{L})\right]\\
&= \frac{1}{n\pi}\left[-\sum_{k=1}^{m-1}\Delta\phi_k\sin\frac{2n\pi l_k}{L}+\sum_{j=1}^{m-1}\Delta\phi_j\sin\frac{2n\pi l_m}{L}\right],\\
\frac{2}{L}\int_0^L \frac{2\pi\lambda}{L}\cos\frac{2n\pi\lambda}{L}d\lambda &= \frac{2}{L}\int_0^L \frac{1}{n}\sin\frac{2n\pi\lambda}{L}d\lambda\\
&= 0.
\end{aligned}
$$

$$
\begin{aligned}
b_n &= \frac{2}{L}\int_0^L \left(\phi(\lambda)+\frac{2\pi\lambda}{L}\right)\sin\frac{2n\pi\lambda}{L}d\lambda,\\
\frac{2}{L}\int_0^L \phi(\lambda)\sin\frac{2n\pi\lambda}{L}d\lambda &= \frac{2}{L}\sum_{k=1}^{m-1}\int_{l_k}^{l_{k+1}}\sum_{j=1}^{l}\Delta\phi_j\sin\frac{2n\pi\lambda}{L}d\lambda\\
&= -\frac{1}{n\pi}\sum_{k=1}^{m-1}\left[\sum_{j=1}^{k}\Delta\phi_j(\cos\frac{2n\pi l_{k+1}}{L}-\cos\frac{2\ \pi l_k}{L})\right]\\
&= -\frac{1}{n\pi}\left[-\sum_{k=1}^{m-1}\Delta\phi_k\cos\frac{2n\pi l_k}{L}+\sum_{j=1}^{m-1}\Delta\phi_j\cos\frac{2n\pi l_m}{L}\right]\\
&= \frac{1}{n\pi}\left[\sum_{k=1}^{m}\Delta\phi_k\cos\frac{2n\pi l_k}{L}-2\pi\right],\\
\frac{2}{L}\int_0^L \frac{2\pi\lambda}{L}\sin\frac{2n\pi\lambda}{L}d\lambda &= \frac{2}{L}\left[\frac{L}{n}-\frac{1}{n}\int_0^L\cos\frac{2n\pi\lambda}{L}d\lambda\right]\\
&= -\frac{2}{n}.
\end{aligned}
$$

B.2 SZR Descriptors

Lemma B.2 *Let γ be a polygonal curve. The Fourier coefficients of $\tilde{\phi}$ are*

$$\begin{aligned}
\tilde{\mu}_0 &= -2\pi - \frac{1}{L'}\sum_{i=1}^{m} l'_i \Delta\phi_i + \frac{\Delta\phi_m}{2}, \\
\tilde{a}_n &= -\frac{1}{n\pi}\left[\frac{L'}{n\pi}\sum_{i=1}^{m-1}\frac{\Delta\phi_i}{\Delta l'_i}\sin\frac{2n\pi l'_i}{L'}\sin\frac{n\pi\Delta l'_i}{L'}\right], \\
\tilde{b}_n &= \frac{1}{n\pi}\left[\frac{L'}{n\pi}\sum_{i=1}^{m-1}\frac{\Delta\phi_i}{\Delta l'_i}\cos\frac{2n\pi l'_i}{L'}\sin\frac{n\pi\Delta l'_i}{L'} + 2\pi\right].
\end{aligned}$$

Proof Let γ' be the quasipolygonal curve corresponding to the smoothed signature $\tilde{\phi}$ with points $V'_0, \ldots, V'_{m-1}$ located in the middle of the circular arcs. The Fourier coefficients of $\tilde{\phi}$ are calculated as follows

$$\tilde{\mu}_0 = \frac{1}{L'}\int_0^{L'} \tilde{\phi}(t)dt = S_1^{\tilde{\mu}_0} + S_2^{\tilde{\mu}_0}$$

where $S_1^{\tilde{\mu}0}$ is the cumulative area under constant pieces of SZR and $S_2^{\tilde{\mu}_0}$ is the cumulative area under linear pieces of SZR. Now

$$\begin{aligned}
S_1^{\tilde{\mu}_0} &= \frac{1}{L'}\left[\int_{\frac{\Delta l'_m}{2}}^{l'_1-\frac{\Delta l'_1}{2}}\frac{\Delta\phi_m}{2}dt + \sum_{i=1}^{m-1}\int_{l'_i+\frac{\Delta l'_i}{2}}^{l'_{i+1}-\frac{\Delta l'_{i+1}}{2}}\left(\frac{\Delta\phi_m}{2} + \sum_{j=1}^{i}\Delta\phi_j\right)dt\right] \\
&= \frac{1}{L'}\left[\frac{\Delta\phi_m}{2}\left(l'_1 - \frac{\Delta l'_1}{2} - \frac{\Delta l'_m}{2}\right) + \right. \\
&\quad \left.\sum_{i=1}^{m-1}\left(\frac{\Delta\phi_m}{2} + \sum_{j=1}^{i}\Delta\phi_j\right)\left(l'_{i+1} - \frac{\Delta l'_{i+1}}{2} - l'_i - \frac{\Delta l'_i}{2}\right)\right] \\
&= \frac{1}{L'}\left[-\frac{\Delta\phi_m}{2}\left(\frac{\Delta l'_1}{2} + \frac{\Delta l'_m}{2}\right) + \frac{\Delta\phi_m}{2}l'_m - \frac{\Delta\phi_m}{2}\sum_{i=1}^{m-1}\left(\frac{\Delta l'_{i+1}}{2} + \frac{\Delta l'_i}{2}\right) - \right. \\
&\quad \left.\sum_{i=1}^{m}\Delta\phi_i l'_i - 2\pi l'_m - \sum_{i=1}^{m-1}\left(\sum_{j=1}^{i}\Delta\phi_j\right)\left(\frac{\Delta l'_{i+1}}{2} + \frac{\Delta l'_i}{2}\right)\right],
\end{aligned}$$

$$\begin{aligned}
S_2^{\tilde{\mu}_0} &= \frac{1}{L'}\left[\int_0^{\frac{\Delta l'_m}{2}}\frac{\Delta\phi_m}{\Delta l'_m}t\,dt + \sum_{i=1}^{m-1}\int_{l'_i-\frac{\Delta l'_i}{2}}^{l'_i+\frac{\Delta l'_i}{2}}\left(\frac{\Delta\phi_i}{\Delta l'_i}t + \frac{\Delta\phi_m}{2} + \frac{\Delta\phi_i}{2} + \right.\right. \\
&\quad \left.\left.\sum_{j=1}^{i-1}\Delta\phi_j - \frac{\Delta\phi_i}{\Delta l'_i}l'_i\right)dt + \int_{l'_m-\frac{\Delta l'_m}{2}}^{l'_m}\left(\frac{\Delta\phi_m}{\Delta l'_m}t - 2\pi - \frac{\Delta\phi_m}{\Delta l'_m}l'_m\right)dt\right]
\end{aligned}$$

$$
\begin{aligned}
&= \frac{1}{L'}\left[\frac{\Delta\phi_m}{\Delta l'_m}(\frac{1}{2})(\frac{\Delta l'_m}{2})^2 + \sum_{i=1}^{m-1}(\frac{\Delta\phi_i}{\Delta l'_i})\frac{t^2}{2}\Big|_{l'_i-\frac{\Delta l'_i}{2}}^{l'_i+\frac{\Delta l'_i}{2}} + \right.\\
&\quad \sum_{i=1}^{m-1}(\frac{\Delta\phi_m}{2} + \frac{\Delta\phi_i}{2} + \sum_{j=1}^{i-1}\Delta\phi_j - \frac{\Delta\phi_i}{\Delta l'_i}l'_i)(\Delta l'_i) + \\
&\quad \left.(\frac{\Delta\phi_m}{\Delta l'_m})(\frac{t^2}{2})\Big|_{l'_m-\frac{\Delta l'_m}{2}}^{l'_m} - (2\pi + \frac{\Delta\phi_m}{\Delta l'_m}l'_m)\frac{\Delta l'_m}{2}\right]\\
&= \frac{1}{L'}\left[\frac{\Delta\phi_m}{8}\Delta l'_m + \sum_{i=1}^{m-1}(\frac{\Delta\phi_i}{\Delta l'_i})l'_i\Delta l'_i + \frac{\Delta\phi_m}{2}\sum_{i=1}^{m-1}\Delta l'_i + \right.\\
&\quad \frac{1}{2}\sum_{i=1}^{m-1}\Delta\phi_i\Delta l'_i + \sum_{i=1}^{m-1}(\sum_{j=1}^{i-1}\Delta\phi_j)\Delta l'_i - \sum_{i=1}^{m-1}\Delta\phi_i l'_i + \\
&\quad \left.(\frac{\Delta\phi_m}{\Delta l'_m})(\frac{1}{2})(l'_m\Delta l'_m - (\frac{\Delta l'_m}{2})^2) - \pi\Delta l'_m - \frac{1}{2}\Delta\phi_m l'_m\right]\\
&= \frac{1}{L'}\left[\frac{\Delta\phi_m}{2}\sum_{i=1}^{m-1}\Delta l'_i + \frac{1}{2}\sum_{i=1}^{m-1}\Delta\phi_i\Delta l'_i + \sum_{i=1}^{m-1}(\sum_{j=1}^{i-1}\Delta\phi_j)\Delta l'_i - \pi\Delta l'_m\right],
\end{aligned}
$$

$$
\begin{aligned}
\tilde{\mu}_0 &= S_1^{\tilde{\mu}_0} + S_2^{\tilde{\mu}_0}\\
&= \frac{1}{L'}\left[-\frac{\Delta\phi_m}{2}(\frac{\Delta l'_1}{2} + \frac{\Delta l'_m}{2}) + \frac{\Delta\phi_m}{2}l'_m - \frac{\Delta\phi_m}{2}\sum_{i=1}^{m-1}(\frac{\Delta l'_{i+1}}{2} + \frac{\Delta l'_i}{2}) - \right.\\
&\quad \sum_{i=1}^{m}\Delta\phi_i l'_i - 2\pi l'_m - \sum_{i=1}^{m-1}(\sum_{j=1}^{i}\Delta\phi_j)(\frac{\Delta l'_{i+1}}{2} + \frac{\Delta l'_i}{2}) + \\
&\quad \left.\frac{\Delta\phi_m}{2}\sum_{i=1}^{m-1}\Delta l'_i + \frac{1}{2}\sum_{i=1}^{m-1}\Delta\phi_i\Delta l'_i + \sum_{i=1}^{m-1}(\sum_{j=1}^{i-1}\Delta\phi_j)\Delta l'_i - \pi\Delta l'_m\right]\\
&= \frac{1}{L'}\left[-\frac{\Delta\phi_m}{2}(\frac{\Delta l'_1}{2} + \frac{\Delta l'_m}{2}) + \frac{\Delta\phi_m}{2}l'_m - \frac{\Delta\phi_m}{4}\sum_{i=1}^{m-1}\Delta l'_{i+1} - \right.\\
&\quad \sum_{i=1}^{m}l'_i\Delta\phi_i - 2\pi l'_m - \frac{1}{2}\sum_{i=1}^{m-1}(\sum_{j=1}^{i}\Delta\phi_j)\Delta l'_{i+1} + \\
&\quad \sum_{i=1}^{m-1}(\sum_{j=1}^{i-1}\Delta\phi_j)\Delta l'_i - \frac{1}{2}\sum_{i=1}^{m-1}(\sum_{j=1}^{i}\Delta\phi_j)\Delta l'_i + \\
&\quad \left.\frac{1}{2}\sum_{i=1}^{m-1}\Delta\phi_i\Delta l'_i + \frac{\Delta\phi_m}{4}\sum_{i=1}^{m-1}\Delta l'_i - \pi\Delta l'_m\right]\\
&= \frac{1}{L'}\left[-\sum_{i=1}^{m}l'_i\Delta\phi_i - 2\pi l'_m + \frac{\Delta\phi_m}{2}l'_m\right].
\end{aligned}
$$

$$\begin{aligned}\tilde{a}_n &= \frac{2}{L'}\int_0^{L'}\tilde{\phi}(t)\cos(\frac{2n\pi}{L'}t)dt \\ &= S_1^{\tilde{a}_n} + S_2^{\tilde{a}_n}\end{aligned}$$

where $S_1^{\tilde{a}_n}$ is the cumulative area under constant pieces of SZR and $S_2^{\tilde{a}_n}$ is the cimulative area under linear pieces of SZR. Now

$$\begin{aligned}S_1^{\tilde{a}_n} &= \frac{2}{L'}\left[\sum_{i=1}^{m-1}\int_{l_i'+\frac{\Delta l_i'}{2}}^{l_{i+1}'-\frac{\Delta l_{i+1}'}{2}}(\frac{\Delta\phi_m}{2}+\sum_{j=1}^{i}\Delta\phi_j)\cos(\frac{2n\pi}{L'}t)dt+\right. \\ &\left.\int_{\frac{\Delta l_m'}{2}}^{l_1'-\frac{\Delta l_1'}{2}}\frac{\Delta\phi_m}{2}\cos(\frac{2n\pi}{L'}t)dt\right] \\ &= \frac{1}{n\pi}\sum_{i=1}^{m-1}(\frac{\Delta\phi_m}{2}+\sum_{j=1}^{i}\Delta\phi_j)\sin(\frac{2n\pi}{L'}t)\Big|_{l_i'+\frac{\Delta l_i'}{2}}^{l_{i+1}'-\frac{\Delta l_{i+1}'}{2}}+\frac{1}{n\pi}\frac{\Delta\phi_m}{2}\sin(\frac{2n\pi}{L'}t)\Big|_{\frac{\Delta l_m'}{2}}^{l_1'-\frac{\Delta l_1'}{2}} \\ &= \frac{1}{n\pi}\left[\sum_{i=1}^{m-1}(\frac{\Delta\phi_m}{2}+\sum_{j=1}^{i}\Delta\phi_j)(\sin\frac{2n\pi}{L'}(l_{i+1}'-\frac{\Delta l_{i+1}'}{2})-\right. \\ &\left.\sin\frac{2n\pi}{L'}(l_i'+\frac{\Delta l_i'}{2}))+\frac{\Delta\phi_m}{2}(\sin\frac{2n\pi}{L'}(l_1'-\frac{\Delta l_1'}{2})-\sin\frac{n\pi}{L'}\Delta l_m')\right] \\ &= \frac{1}{n\pi}\left[-\Delta\phi_m\sum_{i=1}^{m}\cos\frac{2n\pi}{L'}l_i'\sin\frac{n\pi}{L'}\Delta l_i'-\sum_{i=1}^{m-1}\Delta\phi_i\sin\frac{2n\pi}{L'}l_i'\cos\frac{n\pi}{L'}\Delta l_i'-\right. \\ &\left.\sum_{i=1}^{m-1}(\sum_{j=1}^{i}\Delta\phi_j)\cos\frac{2n\pi}{L'}l_{i+1}'\sin\frac{n\pi}{L'}\Delta l_{i+1}'-\sum_{i=1}^{m-1}(\sum_{j=1}^{i}\Delta\phi_j)\cos\frac{2n\pi}{L'}l_i'\sin\frac{n\pi}{L'}\Delta l_i'\right],\end{aligned}$$

$$\begin{aligned}S_2^{\tilde{a}_n} &= \frac{2}{L'}\left[\int_0^{\frac{\Delta\phi_m}{2}}\frac{\Delta\phi_m}{\Delta l_m'}t\cos(\frac{2n\pi}{L'}t)dt+\right. \\ &\sum_{i=1}^{m-1}\int_{l_i'-\frac{\Delta l_i'}{2}}^{l_i'+\frac{\Delta l_i'}{2}}(\frac{\Delta\phi_i}{\Delta l_i'}t+\frac{\Delta\phi_m}{2}+\frac{\Delta\phi_i}{2}+\sum_{j=1}^{i-1}\Delta\phi_j-\frac{\Delta\phi_i}{\Delta l_i'}l_i')\cos(\frac{2n\pi}{L'}t)dt \\ &\left.+\int_{l_m'-\frac{\Delta l_m'}{2}}^{l_m'}(\frac{\Delta\phi_m}{\Delta l_m'}t-2\pi-\frac{\Delta\phi_m}{\Delta l_m'}l_m')\cos(\frac{2n\pi}{L'}t)dt\right] \\ &= \frac{1}{n\pi}\frac{\Delta\phi_m}{\Delta l_m'}\frac{L'}{2n\pi}(\frac{2n\pi}{L'}t\sin\frac{2n\pi}{L'}t+\cos\frac{2n\pi}{L'}t)\Big|_0^{\frac{\Delta l_m'}{2}}+ \\ &\frac{1}{n\pi}\frac{L'}{2n\pi}\sum_{i=1}^{m-1}\frac{\Delta\phi_i}{\Delta l_i'}(\frac{2n\pi}{L'}t\sin\frac{2n\pi}{L'}t+\cos\frac{2n\pi}{L'}t)\Big|_{l_i'-\frac{\Delta l_i'}{2}}^{l_i'+\frac{\Delta l_i'}{2}}+\end{aligned}$$

$$\frac{1}{n\pi}\sum_{i=1}^{m-1}(\frac{\Delta\phi_m}{2}+\frac{\Delta\phi_i}{2}+\sum_{j=1}^{i-1}\Delta\phi_j-\frac{\Delta\phi_i}{\Delta l'_i}l'_i)\sin\frac{2n\pi}{L'}t\Big|_{l'_i-\frac{\Delta l'_i}{2}}^{l'_i+\frac{\Delta l'_i}{2}}+$$

$$\frac{1}{n\pi}\frac{\Delta\phi_m}{\Delta l'_m}\frac{L'}{2n\pi}(\frac{2n\pi}{L'}t\sin\frac{2n\pi}{L'}t+\cos\frac{2n\pi}{L'}t)\Big|_{l'_m-\frac{\Delta l'_m}{2}}^{l'_m}-$$

$$\frac{1}{n\pi}(2\pi+\frac{\Delta\phi_m}{\Delta l'_m}l'_m)\sin\frac{2n\pi}{L'}t\Big|_{l'_m-\frac{\Delta l'_m}{2}}^{l'_m}$$

$$=\frac{1}{n\pi}\Bigg[\frac{\Delta\phi_m}{\Delta l'_m}\frac{L'}{2n\pi}(\frac{n\pi}{L'}\Delta l'_m\sin\frac{n\pi}{L'}\Delta l'_m+\cos\frac{n\pi}{L'}\Delta l'_m-1)+$$

$$\frac{L'}{2n\pi}\sum_{i=1}^{m-1}\frac{\Delta\phi_i}{\Delta l'_i}(\frac{2n\pi}{L'}(l'_i+\frac{\Delta l'_i}{2})\sin\frac{2n\pi}{L'}(l'_i+\frac{\Delta l'_i}{2})+\cos\frac{2n\pi}{L'}(l'_i+\frac{\Delta l'_i}{2}))-$$

$$\frac{L'}{2n\pi}\sum_{i=1}^{m-1}\frac{\Delta\phi_i}{\Delta l'_i}(\frac{2n\pi}{L'}(l'_i-\frac{\Delta l'_i}{2})\sin\frac{2n\pi}{L'}(l'_i-\frac{\Delta l'_i}{2})+\cos\frac{2n\pi}{L'}(l'_i-\frac{\Delta l'_i}{2}))+$$

$$\sum_{i=1}^{m-1}(\frac{\Delta\phi_m}{2}+\frac{\Delta\phi_i}{2}+\sum_{j=1}^{i-1}\Delta\phi_j-\frac{\Delta\phi_i}{\Delta l'_i}l'_i)(\sin\frac{2n\pi}{L'}(l'_i+\frac{\Delta l'_i}{2})-$$

$$\sin\frac{2n\pi}{L'}(l'_i-\frac{\Delta l'_i}{2}))+\frac{\Delta\phi_m}{\Delta l'_m}\frac{L'}{2n\pi}(\frac{2n\pi}{L'}l'_m\sin\frac{2n\pi}{L'}l'_m+1)-$$

$$\frac{\Delta\phi_m}{\Delta l'_m}\frac{L'}{2n\pi}(\frac{2n\pi}{L'}(l'_m-\frac{\Delta l'_m}{2})\sin\frac{2n\pi}{L'}(l'_m-\frac{\Delta l'_m}{2})+$$

$$\cos\frac{2n\pi}{L'}(l'_m-\frac{\Delta l'_m}{2}))-(2\pi+\frac{\Delta\phi_m}{\Delta l'_m}l'_m)(\sin\frac{2n\pi}{L'}l'_m-\sin\frac{2n\pi}{L'}(l'_m-\frac{\Delta l'_m}{2}))\Bigg]$$

$$=\frac{1}{n\pi}\Bigg[\sum_{i=1}^{m-1}\Delta\phi_i\sin\frac{2n\pi}{L'}l'_i\cos\frac{n\pi}{L'}\Delta l'_i+\sum_{i=1}^{m-1}\Delta\phi_i\cos\frac{2n\pi}{L'}l'_i\sin\frac{n\pi}{L'}\Delta l'_i-$$

$$2\pi\sin\frac{n\pi}{L'}\Delta l'_m-\frac{L'}{n\pi}\sum_{i=1}^{m-1}\frac{\Delta\phi_i}{\Delta l'_i}\sin\frac{2n\pi}{L'}l'_i\sin\frac{n\pi}{L'}\Delta l'_i+$$

$$\Delta\phi_m\sum_{i=1}^{m-1}\cos\frac{2n\pi}{L'}l'_i\sin\frac{n\pi}{L'}\Delta l'_i+2\sum_{i=1}^{m-1}(\sum_{j=1}^{i-1}\Delta\phi_j)\cos\frac{2n\pi}{L'}l'_i\sin\frac{n\pi}{L'}\Delta l'_i\Bigg],$$

$$\tilde{a}_n=S_1^{\tilde{a}_n}+S_2^{\tilde{a}_n}$$

$$=\frac{1}{n\pi}\Bigg[-\Delta\phi_m\sum_{i=1}^{m}\cos\frac{2n\pi}{L'}l'_i\sin\frac{n\pi}{L'}\Delta l'_i-\sum_{i=1}^{m-1}\Delta\phi_i\sin\frac{2n\pi}{L'}l'_i\cos\frac{n\pi}{L'}\Delta l'_i$$

$$-\sum_{i=1}^{m-1}(\sum_{j=1}^{i}\Delta\phi_j)\cos\frac{2n\pi}{L'}l'_{i+1}\sin\frac{n\pi}{L'}\Delta l'_{i+1}-$$

$$\sum_{i=1}^{m-1}(\sum_{j=1}^{i}\Delta\phi_j)\cos\frac{2n\pi}{L'}l'_i\sin\frac{n\pi}{L'}\Delta l'_i+\sum_{i=1}^{m-1}\Delta\phi_i\sin\frac{2n\pi}{L'}l'_i\cos\frac{n\pi}{L'}\Delta l'_i+$$

$$\sum_{i=1}^{m-1} \Delta\phi_i \cos\frac{2n\pi}{L'} l'_i \sin\frac{n\pi}{L'}\Delta l'_i - 2\pi \sin\frac{n\pi}{L'}\Delta l'_m -$$
$$\frac{L'}{n\pi}\sum_{i=1}^{m-1}\frac{\Delta\phi_i}{\Delta l'_i}\sin\frac{2n\pi}{L'} l'_i \sin\frac{n\pi}{L'}\Delta l'_i + \Delta\phi_m \sum_{i=1}^{m-1}\cos\frac{2n\pi}{L'}\sin\frac{n\pi}{L'}\Delta l'_i +$$
$$2\sum_{i=1}^{m-1}\Big(\sum_{j=1}^{i-1}\Delta\phi_j\Big)\cos\frac{2n\pi}{L'} l'_i \sin\frac{n\pi}{L'}\Delta l'_i\Bigg]$$

$$= \frac{1}{n\pi}\Bigg[-\Delta\phi_m \sum_{i=1}^{m-1}\cos\frac{2n\pi}{L'} l'_i \sin\frac{n\pi}{L'}\Delta l'_i - \Delta\phi_m \cos\frac{2n\pi}{L'} l'_m \sin\frac{n\pi}{L'}\Delta l'_m -$$
$$\sum_{i=1}^{m-1}\Big(\sum_{j=1}^{i}\Delta\phi_j\Big)\cos\frac{2n\pi}{L'} l'_{i+1}\sin\frac{n\pi}{L'}\Delta l'_{i+1} +$$
$$\sum_{i=1}^{m-1}\Big(\sum_{j=1}^{i-1}\Delta\phi_j\Big)\cos\frac{2n\pi}{L'} l'_i \sin\frac{n\pi}{L'}\Delta l'_i -$$
$$2\pi \sin\frac{n\pi}{L'}\Delta l'_m - \frac{L'}{n\pi}\sum_{i=1}^{m-1}\frac{\Delta\phi_i}{\Delta l'_i}\sin\frac{2n\pi}{L'} l'_i \sin\frac{n\pi}{L'}\Delta l'_i +$$
$$\Delta\phi_m \sum_{i=1}^{m-1}\cos\frac{2n\pi}{L'} l'_i \sin\frac{n\pi}{L'}\Delta l'_i\Bigg]$$

$$= -\frac{1}{n\pi}\left[\frac{L'}{n\pi}\sum_{i=1}^{m-1}\frac{\Delta\phi_i}{\Delta l'_i}\sin\frac{2n\pi}{L'} l'_i \sin\frac{n\pi}{L'}\Delta l'_i\right].$$

$$\begin{aligned}\tilde{b}_n &= \frac{2}{L'}\int_0^{L'}\tilde{\phi}(t)\sin(\frac{2n\pi}{L'}t)dt \\ &= S_1^{\tilde{b}_n} + S_2^{\tilde{b}_n}\end{aligned}$$

where $S_1^{\tilde{b}}$ is the cumulative area under constant pieces of SZR and $S_2^{\tilde{b}_n}$ is the cimulative area under linear pieces of SZR. Now

$$\begin{aligned}S_1^{\tilde{b}_n} &= \frac{2}{L'}\left[\int_{\frac{\Delta l'_m}{2}}^{l'_1-\frac{\Delta l'_1}{2}}\frac{\Delta\phi_m}{2}\sin(\frac{2n\pi}{L'}t)dt+\right. \\ &\left.\sum_{i=1}^{m-1}\int_{l'_i+\frac{\Delta l'_i}{2}}^{l'_{i+1}-\frac{\Delta l'_{i+1}}{2}}(\frac{\Delta\phi_m}{2}+\sum_{j=1}^{i}\Delta\phi_j)\sin(\frac{2n\pi}{L'}t)dt\right] \\ &= \frac{1}{n\pi}\frac{\Delta\phi_m}{2}(-\cos\frac{2n\pi}{L'}t)\Big|_{\frac{\Delta l'_m}{2}}^{l'_1-\frac{\Delta l'_1}{2}}+ \\ &\frac{1}{n\pi}\sum_{i=1}^{m-1}(\frac{\Delta\phi_m}{2}+\sum_{j=1}^{i}\Delta\phi_j)(-\cos\frac{2n\pi}{L'}t)\Big|_{l'_i+\frac{\Delta l'_i}{2}}^{l'_{i+1}-\frac{\Delta l'_{i+1}}{2}} \\ &= \frac{1}{n\pi}\left[\frac{\Delta\phi_m}{2}(\cos\frac{n\pi}{L'}\Delta l'_m-\cos\frac{2n\pi}{L'}(l'_1-\frac{\Delta l'_1}{2}))+\right. \\ &\left.\sum_{i=1}^{m-1}(\frac{\Delta\phi_m}{2}+\sum_{j=1}^{i}\Delta\phi_j)(\cos\frac{2n\pi}{L'}(l'_i+\frac{\Delta l'_i}{2})-\cos\frac{2n\pi}{L'}(l'_{i+1}-\frac{\Delta l'_{i+1}}{2})\right] \\ &= \frac{1}{n\pi}\left[-\Delta\phi_m\sum_{i=1}^{m}\sin\frac{2n\pi}{L'}l'_i\sin\frac{n\pi}{L'}\Delta l'_i+\sum_{i=1}^{m}\Delta\phi_i\cos\frac{2n\pi}{L'}l'_i\cos\frac{n\pi}{L'}\Delta l'_i+\right. \\ &2\pi\cos\frac{n\pi}{L'}\Delta l'_m-\sum_{i=1}^{m-1}(\sum_{j=1}^{i}\Delta\phi_j)\sin\frac{2n\pi}{L'}l'_i\sin\frac{n\pi}{L'}\Delta l'_i- \\ &\left.\sum_{i=1}^{m-1}(\sum_{j=1}^{i}\Delta\phi_j)\sin\frac{2n\pi}{L'}l'_{i+1}\sin\frac{n\pi}{L'}\Delta l'_{i+1}\right],\end{aligned}$$

$$\begin{aligned}S_2^{\tilde{b}_n} &= \frac{2}{L'}\left[\int_0^{\frac{\Delta l'_m}{2}}\frac{\Delta\phi_m}{\Delta l'_m}t\sin(\frac{2n\pi}{L'}t)dt+\right. \\ &\sum_{i=1}^{m-1}\int_{l'_i-\frac{\Delta l'_i}{2}}^{l'_i+\frac{\Delta l'_i}{2}}(\frac{\Delta\phi_i}{\Delta l'_i}t+\frac{\Delta\phi_m}{2}+\frac{\Delta\phi_i}{2}+\sum_{j=1}^{i-1}\Delta\phi_j-\frac{\Delta\phi_i}{\Delta l'_i}l'_i)\sin(\frac{2n\pi}{L'}t)dt \\ &\left.\int_{l'_m-\frac{\Delta l'_m}{2}}^{l'_m}(\frac{\Delta\phi_m}{\Delta l'_m}t-2\pi-\frac{\Delta\phi_m}{\Delta l'_m}l'_m)\sin(\frac{2n\pi}{L'}t)dt\right]\end{aligned}$$

$$
\begin{aligned}
= \quad & \frac{1}{n\pi}\frac{\Delta\phi_m}{\Delta l'_m}\frac{L'}{2n\pi}(\sin\frac{2n\pi}{L'}t - \frac{2n\pi}{L'}t\cos\frac{2n\pi}{L'}t)\Big|_0^{\frac{\Delta l'_m}{2}} + \\
& \frac{1}{n\pi}\frac{L'}{2n\pi}\sum_{i=1}^{m-1}\frac{\Delta\phi_i}{\Delta l'_i}(\sin\frac{2n\pi}{L'}t - \frac{2n\pi}{L'}t\cos\frac{2n\pi}{L'}t)\Big|_{l'_i-\frac{\Delta l'_i}{2}}^{l'_i+\frac{\Delta l'_i}{2}} + \\
& \frac{1}{n\pi}\sum_{i=1}^{m-1}(\frac{\Delta\phi_m}{2}+\frac{\Delta\phi_i}{2}+\sum_{j=1}^{i-1}\Delta\phi_j - \frac{\Delta\phi_i}{\Delta l'_i}l'_i)(-\cos\frac{2n\pi}{L'}t)\Big|_{l'_i-\frac{\Delta l'_i}{2}}^{l'_i+\frac{\Delta l'_i}{2}} + \\
& \frac{1}{n\pi}\frac{L'}{2n\pi}\frac{\Delta\phi_m}{\Delta l'_m}(\sin\frac{2n\pi}{L'}t - \frac{2n\pi}{L'}t\cos\frac{2n\pi}{L'}t)\Big|_{l'_m-\frac{\Delta l'_m}{2}}^{l'_m} - \\
& (2\pi+\frac{\Delta\phi_m}{\Delta l'_m}l'_m)(-\cos\frac{2n\pi}{L'}t)\Big|_{l'_m-\frac{\Delta l'_m}{2}}^{l'_m} \\
= \quad & \frac{1}{n\pi}\Big[\frac{\Delta\phi_m}{\Delta l'_m}\frac{L'}{2n\pi}(\sin\frac{n\pi}{L'}\Delta l'_m - \frac{n\pi}{L'}\Delta l'_m\cos\frac{n\pi}{L'}\Delta l'_m)+ \\
& \frac{L'}{2n\pi}\sum_{i=1}^{m-1}\frac{\Delta\phi_i}{\Delta l'_i}(\sin\frac{2n\pi}{L'}(l'_i+\frac{\Delta l'_i}{2}) - \frac{2n\pi}{L'}(l'_i+\frac{\Delta l'_i}{2})\cos\frac{2n\pi}{L'}(l'_i+\frac{\Delta l'_i}{2}) \\
& \quad -\sin\frac{2n\pi}{L'}(l'_i-\frac{\Delta l'_i}{2}) + \frac{2n\pi}{L'}(l'_i-\frac{\Delta l'_i}{2})\cos\frac{2n\pi}{L'}(l'_i-\frac{\Delta l'_i}{2})) + \\
& \sum_{i=1}^{m-1}(\frac{\Delta\phi_m}{2}+\frac{\Delta\phi_i}{2}+\sum_{j=1}^{i-1}\Delta\phi_j - \frac{\Delta\phi_i}{\Delta l'_i}l'_i) \\
& \quad (\cos\frac{2n\pi}{L'}(l'_i-\frac{\Delta l'_i}{2}) - \cos\frac{2n\pi}{L'}(l'_i+\frac{\Delta l'_i}{2})) + \\
& \frac{\Delta\phi_m}{\Delta l'_m}\frac{L'}{2n\pi}(\sin\frac{2n\pi}{L'}l'_m - \frac{2n\pi}{L'}l'_m\cos\frac{2n\pi}{L'}l'_m - \\
& \sin\frac{2n\pi}{L'}(l'_m-\frac{\Delta l'_m}{2})+\frac{2n\pi}{L'}(l'_m-\frac{\Delta l'_m}{2})\cos\frac{2n\pi}{L'}(l'_m-\frac{\Delta l'_m}{2})) - \\
& (2\pi+\frac{\Delta\phi_m}{\Delta l'_m}l'_m)(\cos\frac{2n\pi}{L'}(l'_m-\frac{\Delta l'_m}{2}) - \cos\frac{2n\pi}{L'}l'_m)\Big] \\
= \quad & \frac{1}{n\pi}\Big[\frac{L'}{n\pi}\sum_{i=1}^{m}\frac{\Delta\phi_i}{\Delta l'_i}\cos\frac{2n\pi}{L'}l'_i\sin\frac{n\pi}{L'}\Delta l'_i + 2\pi - \\
& \sum_{i=1}^{m}\Delta\phi_i\cos\frac{2n\pi}{L'}l'_i\cos\frac{n\pi}{L'}\Delta l'_i + \Delta\phi_m\sum_{i=1}^{m-1}\sin\frac{2n\pi}{L'}l'_i\sin\frac{n\pi}{L'}\Delta l'_i + \\
& 2\sum_{i=1}^{m-1}(\sum_{j=1}^{i-1}\Delta\phi_j)\sin\frac{2n\pi}{L'}l'_i\sin\frac{n\pi}{L'}\Delta l'_i - 2\pi\cos\frac{n\pi}{L'}\Delta l'_m + \\
& \sum_{i=1}^{m-1}\Delta\phi_i\sin\frac{2n\pi}{L'}l'_i\sin\frac{n\pi}{L'}\Delta l'_i\Big],
\end{aligned}
$$

$$
\begin{aligned}
\tilde{b}_n &= S_1^{\tilde{b}_n} + S_2^{\tilde{b}_n} \\
&= \frac{1}{n\pi}\left[-\Delta\phi_m \sum_{i=1}^{m} \sin\frac{2n\pi}{L'} l'_i \sin\frac{n\pi}{L'}\Delta l'_i + \sum_{i=1}^{m} \Delta\phi_i \cos\frac{2n\pi}{L'} l'_i \cos\frac{n\pi}{L'}\Delta l'_i + \right. \\
&\quad 2\pi \cos\frac{n\pi}{L'}\Delta l'_m - \sum_{i=1}^{m-1}\left(\sum_{j=1}^{i}\Delta\phi_j\right) \sin\frac{2n\pi}{L'} l'_i \sin\frac{n\pi}{L'}\Delta l'_i - \\
&\quad \sum_{i=1}^{m-1}\left(\sum_{j=1}^{i}\Delta\phi_j\right) \sin\frac{2n\pi}{L'} l'_{i+1} \sin\frac{n\pi}{L'}\Delta l'_{i+1} + 2\pi + \\
&\quad \frac{L'}{n\pi}\sum_{i=1}^{m}\frac{\Delta\phi_i}{\Delta l'_i} \cos\frac{2n\pi}{L'} l'_i \sin\frac{n\pi}{L'}\Delta l'_i - 2\pi \cos\frac{n\pi}{L'}\Delta l'_m - \\
&\quad \sum_{i=1}^{m}\Delta\phi_i \cos\frac{2n\pi}{L'} l'_i \cos\frac{n\pi}{L'}\Delta l'_i + \Delta\phi_m \sum_{i=1}^{m-1} \sin\frac{2n\pi}{L'} l'_i \sin\frac{n\pi}{L'}\Delta l'_i + \\
&\quad \left. 2\sum_{i=1}^{m-1}\left(\sum_{j=1}^{i-1}\Delta\phi_j\right) \sin\frac{2n\pi}{L'} l'_i \sin\frac{n\pi}{L'}\Delta l'_i + \sum_{i=1}^{m-1}\Delta\phi_i \sin\frac{2n\pi}{L'} l'_i \sin\frac{n\pi}{L'}\Delta l'_i\right] \\
&= \frac{1}{n\pi}\left[\frac{L'}{n\pi}\sum_{i=1}^{m}\frac{\Delta\phi_i}{\Delta l'_i} \cos\frac{2n\pi}{L'} l'_i \sin\frac{n\pi}{L'}\Delta l'_i + 2\pi - \right. \\
&\quad \sum_{i=1}^{m-1}\left(\sum_{j=1}^{i}\Delta\phi_j\right) \sin\frac{2n\pi}{L'} l'_i \sin\frac{n\pi}{L'}\Delta l'_i + \sum_{i=1}^{m-1}\left(\sum_{j=1}^{i-1}\Delta\phi_j\right) \sin\frac{2n\pi}{L'} l'_i \sin\frac{n\pi}{L'}\Delta l'_i - \\
&\quad \sum_{i=1}^{m-1}\left(\sum_{j=1}^{i}\Delta\phi_j\right) \sin\frac{2n\pi}{L'} l'_{i+1} \sin\frac{n\pi}{L'}\Delta l'_{i+1} + \\
&\quad \left. \sum_{i=1}^{m-1}\left(\sum_{j=1}^{i-1}\Delta\phi_j\right) \sin\frac{2n\pi}{L'} l'_i \sin\frac{n\pi}{L'}\Delta l'_i + \sum_{i=1}^{m-1}\Delta\phi_i \sin\frac{2n\pi}{L'} l'_i \sin\frac{n\pi}{L'}\Delta l'_i\right] \\
&= \frac{1}{n\pi}\left[\frac{L'}{n\pi}\sum_{i=1}^{m}\frac{\Delta\phi_i}{\Delta l'_i} \cos\frac{2n\pi}{L'} l'_i \sin\frac{n\pi}{L'}\Delta l'_i + 2\pi\right].
\end{aligned}
$$